Pulsating variables in the classical instability strip

V. Ripepi – INAF Osservatorio Astronomico di Capodimonte

Pulsating variable stars

Pulsating stars are intrinsic variables showing cyclic or periodic variations on a time scale of the order of the *free fall* time $t_{ff}=\sqrt{\frac{3\,\pi}{16\,G\,\rho}}$ (for the Sun ~1 h).

In the simplest case they are <u>radial</u> pulsators.

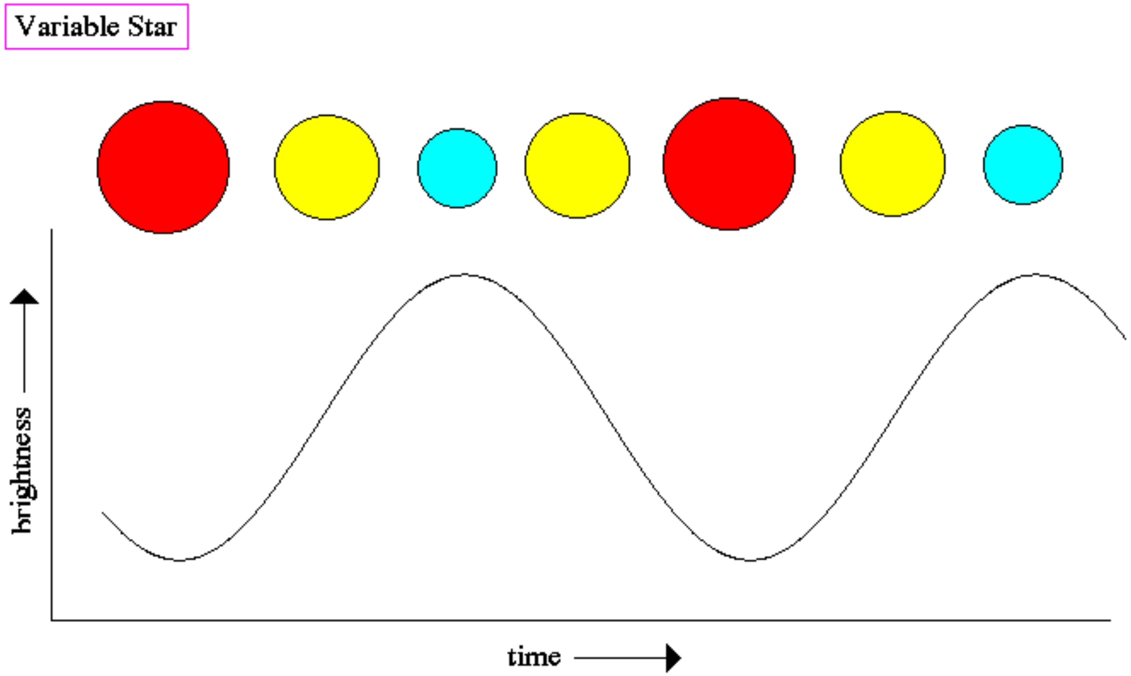

A simple model of pulsation

- Arthur Eddington proposed a model in which pulsating stars act as thermodynamic heat engines. Then radial oscillations can be the result of sound waves resonating in the stellar interior.
- pulsation period, Π, → time it would require a sound wave to travel across the diameter of an ideal star with constant density $\boldsymbol{\rho}$.

- Calling $\boldsymbol{R}$ the radius of the star and $\boldsymbol{v_S}$ the speed of sound we have: $\boldsymbol{\Pi} = \frac{\mathbf{2}\boldsymbol{R}}{\mathbf{v_S}}$ →

$$\Pi \approx \sqrt{\frac{3\pi}{2\gamma G\rho}}$$

Represent the period-mean density relation → Denser stars have smaller periods.
We can estimate roughly the typical periods for star of extreme densities.

$10^6 \geq \rho/\rho_\odot \geq 10^{-9}$ $(\rho_\odot \sim 1.41\ \mathrm{g/cm^3})$

↑ white dwarfs ↑ red supergiants

$\Rightarrow\ 3\ \mathrm{s} \leq \Pi \leq 1000\ \mathrm{d}$

Pulsating stars across the HR diagram

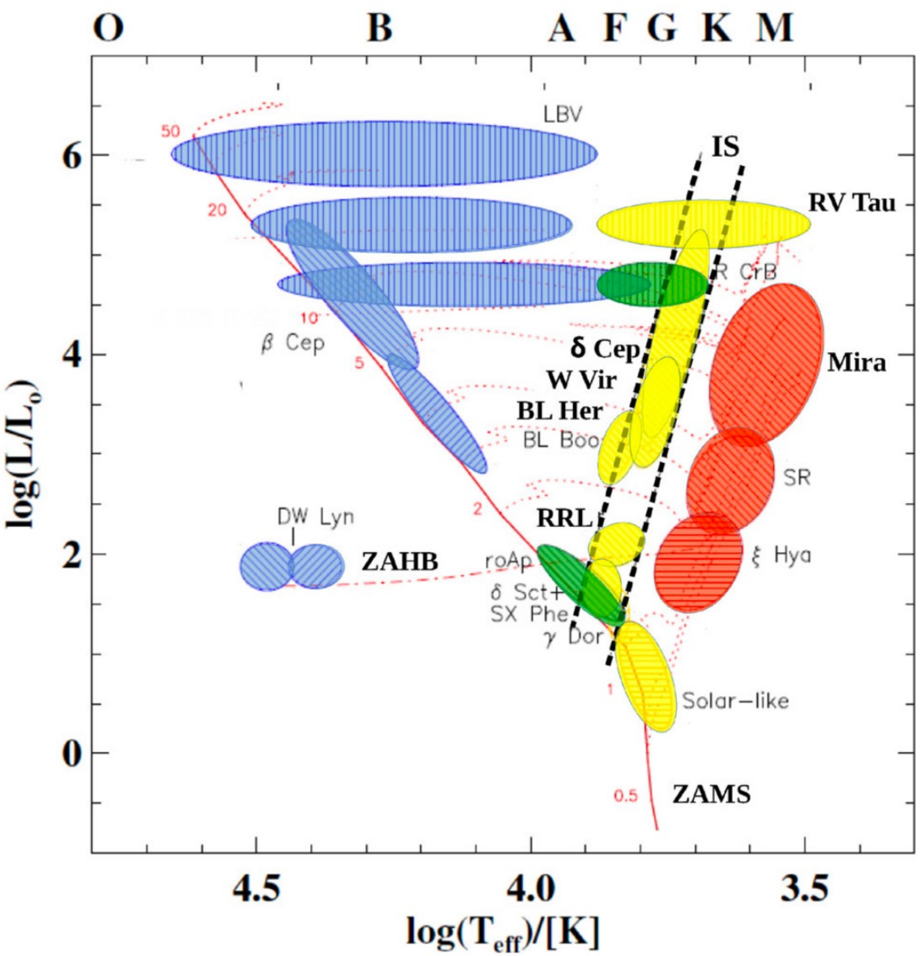

- **Pulsating variable stars provide additional observables such as period(s) and amplitude(s) which can provide constraints on the main stellar parameters (L, Te, M).**

- Periods (and amplitudes) are usually easy to measure with great precision and without the typical uncertainties of photometry and spectroscopy (reddening calibrations etc.).

- Ubiquitous in the HR diagram → constraints on a variety of different type of stars.

- Most useful pulsating stars: **Cepheids (Classical, type II, Anomalous) and RR Lyrae**. They are luminous and with high-amplitude of light variations → easy to detect even at large distances → **distance indicators and stellar population tracers**

Metallicity: definitions

The iron abundance is noted as the logarithm of the ratio of a star's iron abundance compared to that of the Sun:

$$[\mathrm{Fe/H}] = \log_{10}\left(\frac{N_{\mathrm{Fe}}}{N_{\mathrm{H}}}\right)_{\mathrm{star}} - \log_{10}\left(\frac{N_{\mathrm{Fe}}}{N_{\mathrm{H}}}\right)_{\mathrm{sun}},$$

where N_{Fe} and N_{H} are the number of iron and hydrogen atoms per unit of volume respectively.

$[\mathrm{O/H}] \equiv A(\mathrm{O})_{\star} - A(\mathrm{O})_{\odot}$

$A(\mathrm{O}) = \log(N_{\mathrm{O}}/N_{\mathrm{H}}) + 12$

$A(\mathrm{O}) = 8.69$ (Asplund+2009).

$[\mathrm{O/H}] \simeq [\mathrm{Fe/H}]+0.09$ dex for $[\mathrm{Fe/H}] \sim -0.4$ dex (Romaniello+2022)

Z is the per cent abundance of metals: $\log Z = [\mathrm{Fe/H}] - 1.68$

Y is the per cent abundance of Helium

RR Lyrae

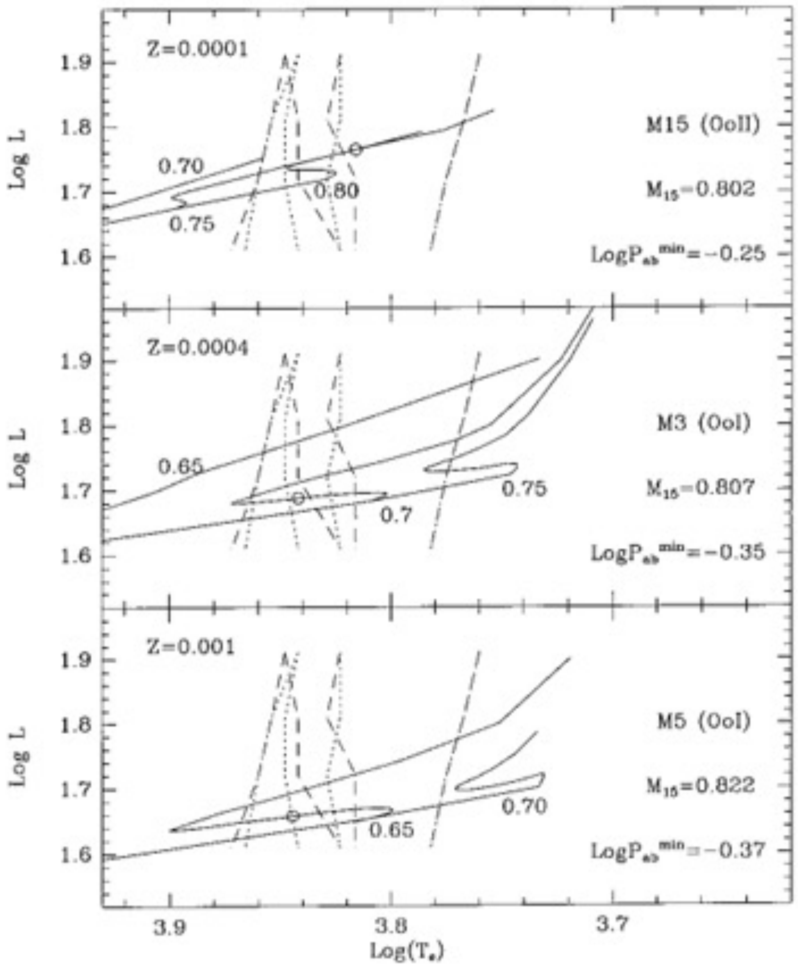

Central helium burning stars. Typical HB stars in Globular clusters

Old (t > 10 Gyrs), low mass ~0.55-0.8 $M_{\odot}$

M_V ~ 0.5-0.6 mag

Periods ~0.2 – 1 d

Amplitudes up to 1.5 mag (optical).

RR Lyrae

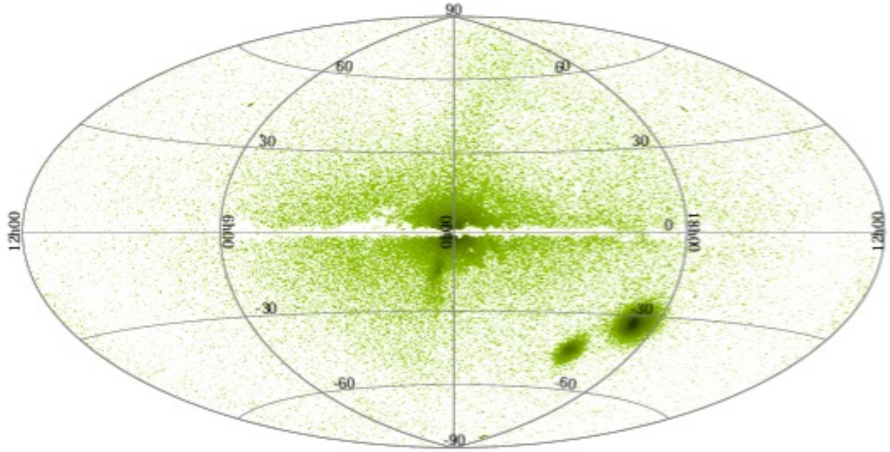

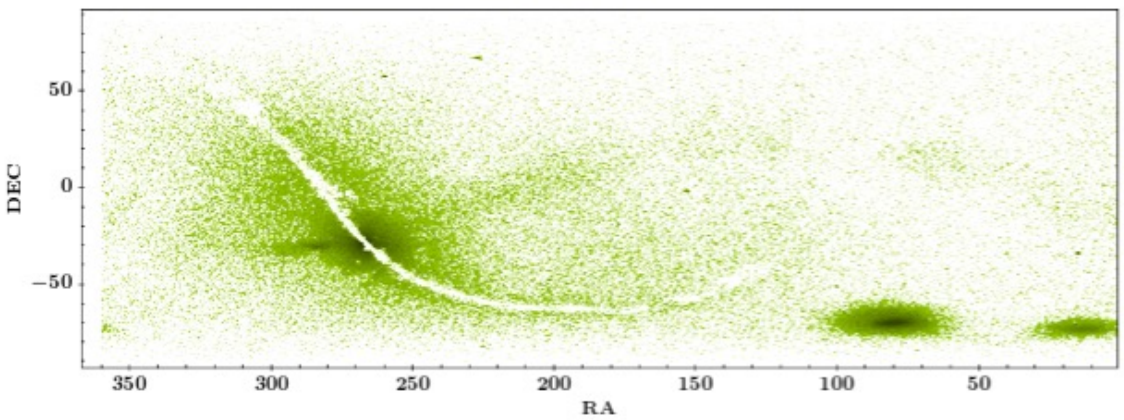

Clementini+2023

- RR Lyrae are ubiquitous variables
- Present where there is an old population → everywhere

RR Lyrae

RRab (Fundamental mode)

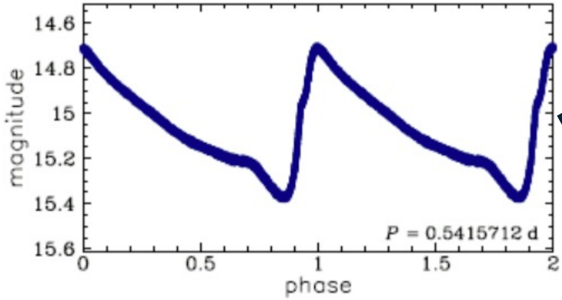

RRc (First overtone mode)

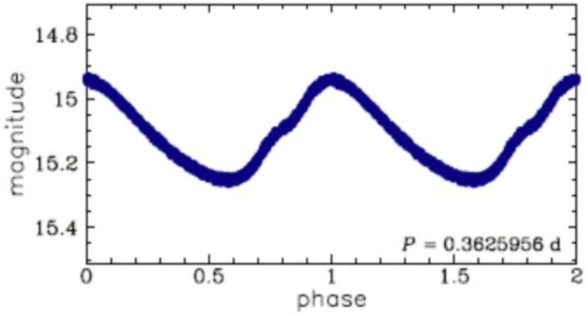

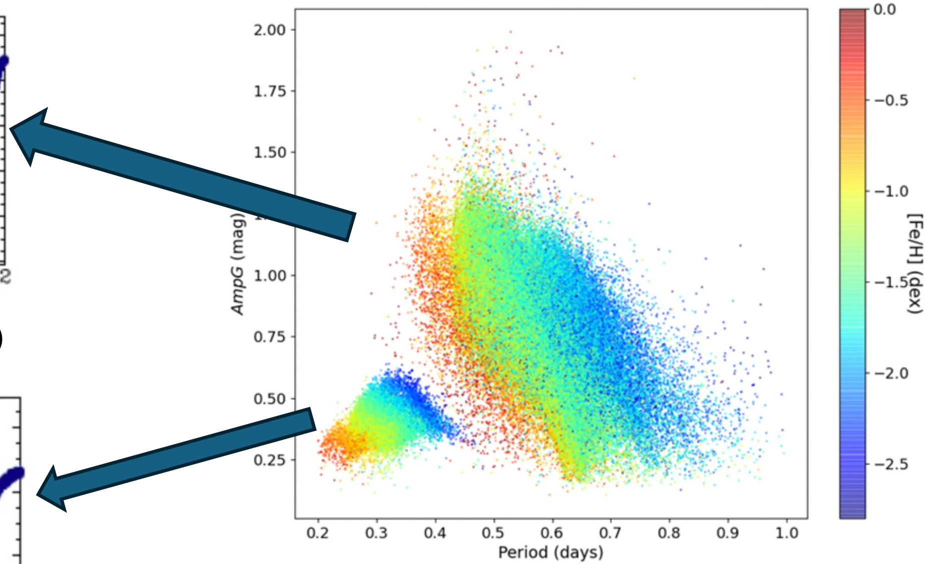

Muraveva+2024

RRd (Mixed mode)

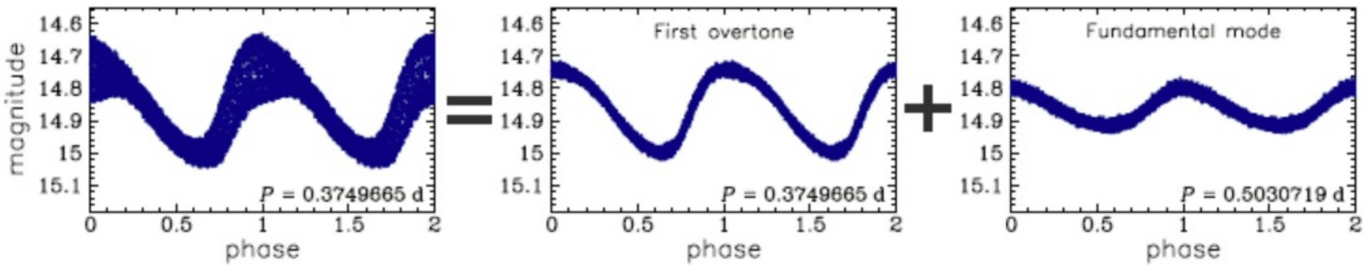

Lower amplitudes in the NIR bands

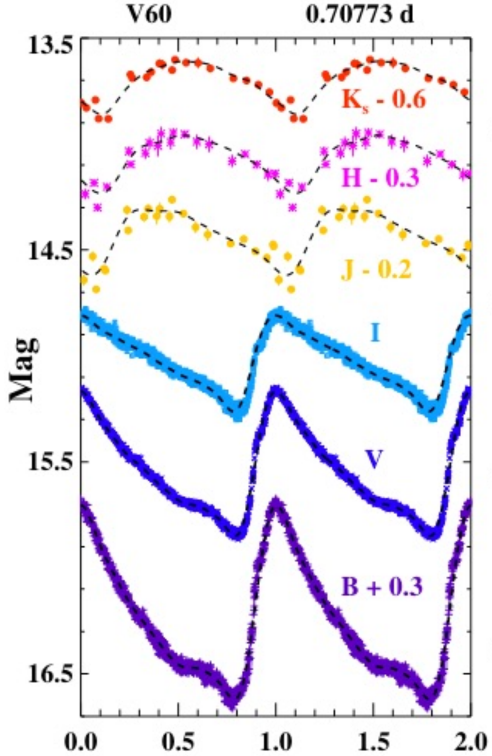

Bhardwaj+2022

A second explanation (van Albada & Baker 1973; Caputo et al. 1987; Bono et al. 1995) relies on an analysis of the instability strip shape.

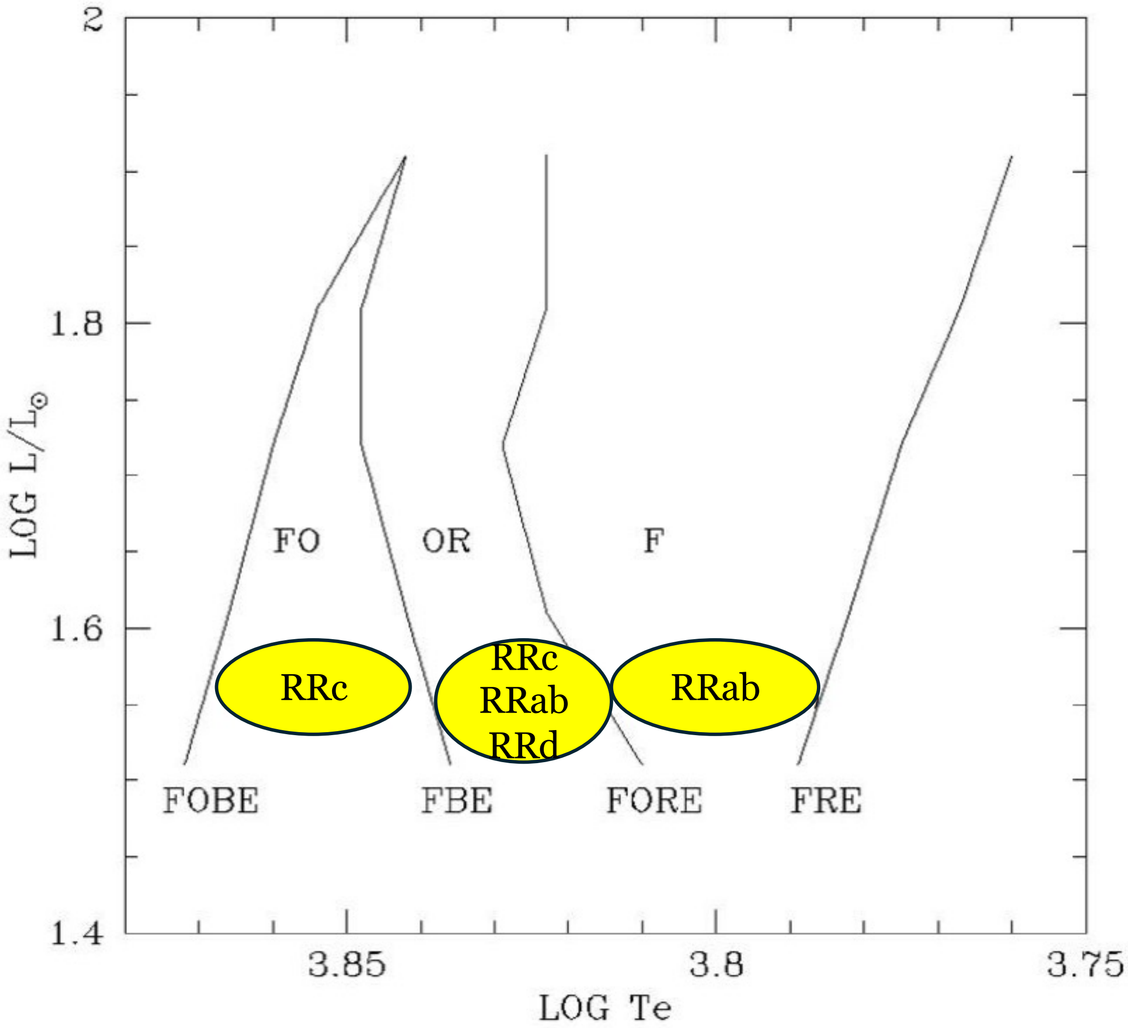

RR Lyrae instability strip

RR Lyrae

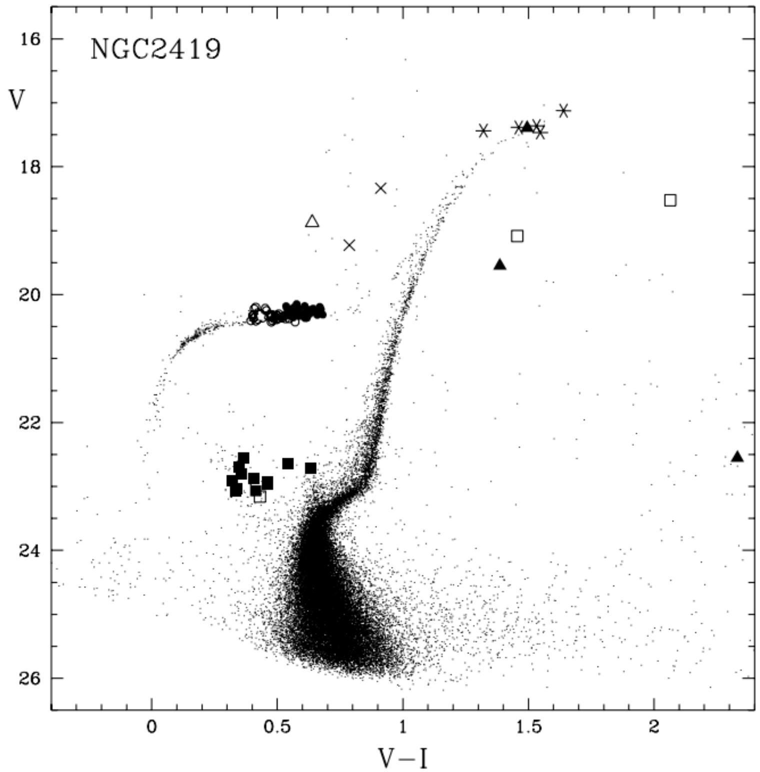

Di Criscienzo+2011

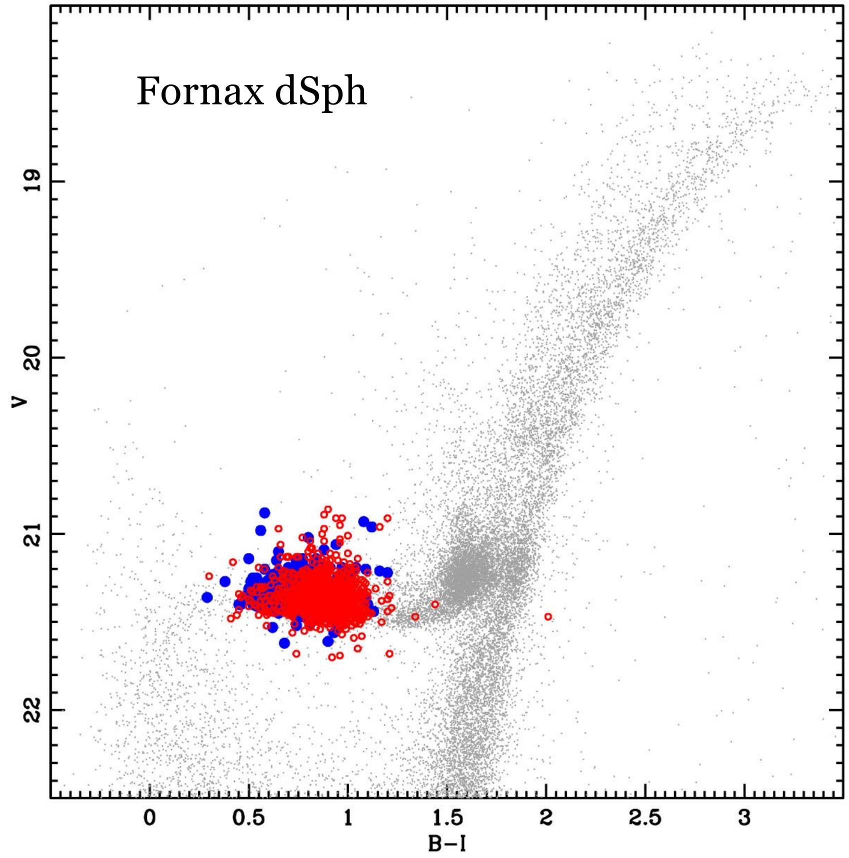

Fiorentino+2015

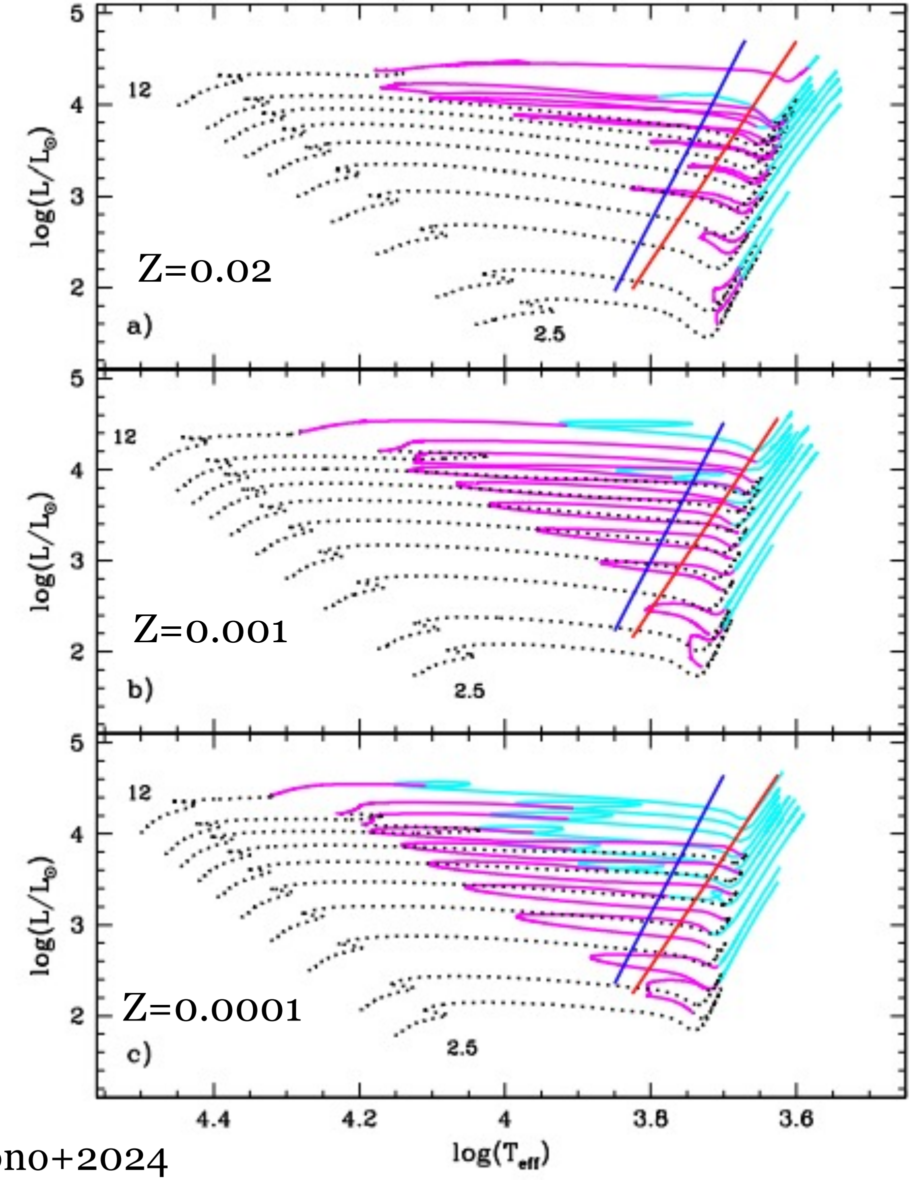

Bono+2024

Classical Cepheids

Classical Cepheids:

Central helium burning stars ($M=3\div13M_\odot$, $M_V= -2\div-7$ mag, $P=1\div100$ d; 50÷500 Myrs).
Pulsate in F, 1O, 2O, Multiple modes.

High amplitudes of variations in the optical (~ 1 mag) → easy to identify even at long distances.

Sufficiently bright to be visible up to ~30 Mpc with HST

Cepheids in the MW and Magellanic Clouds

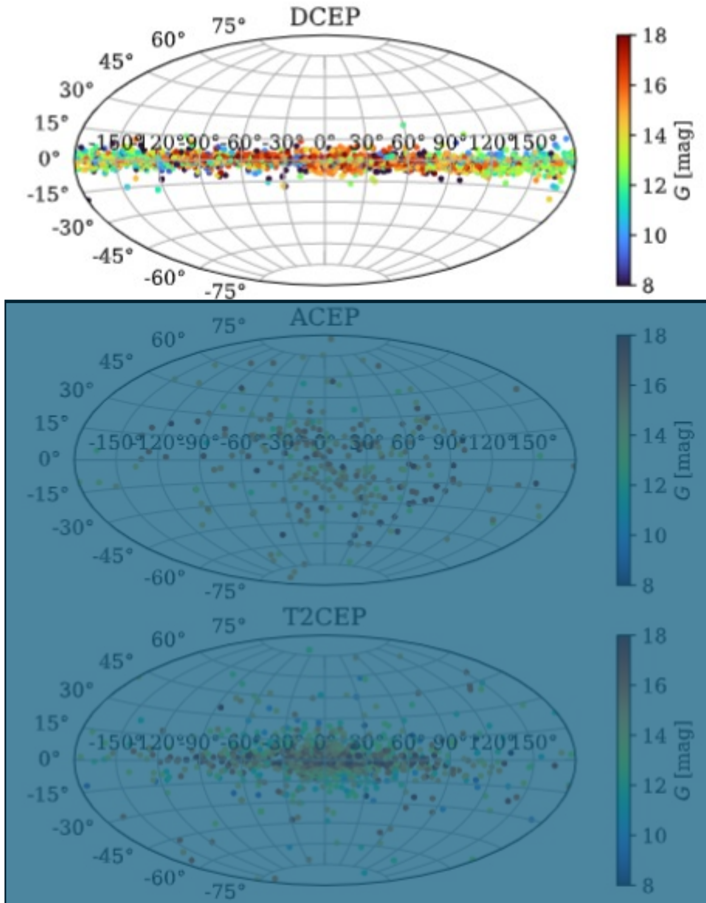

3,434 MW **Classical Cepheids** in Gaia DR3 → largest homogeneous dataset published so far.

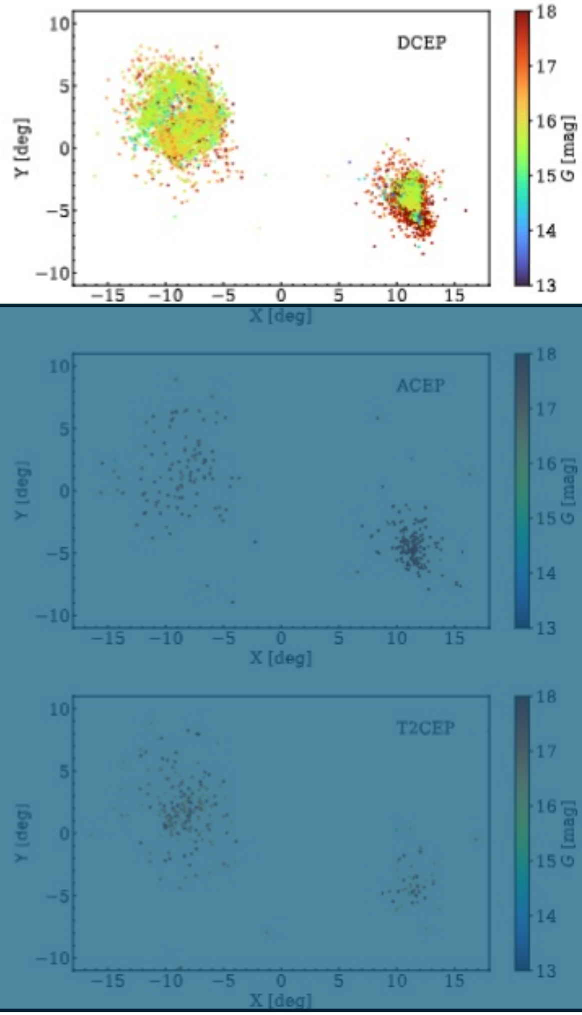

~9,000 Cepheids in the Magellanic Clouds

Ripepi et al. 2023

At the extreme possibility of Gaia: Cepheids in M31 and M33

319 Cepheids in Andromeda (M31 ~ 0.750 Mpc)

185 Cepheids in Triangulum (M33 ~ 0.840 Mpc)

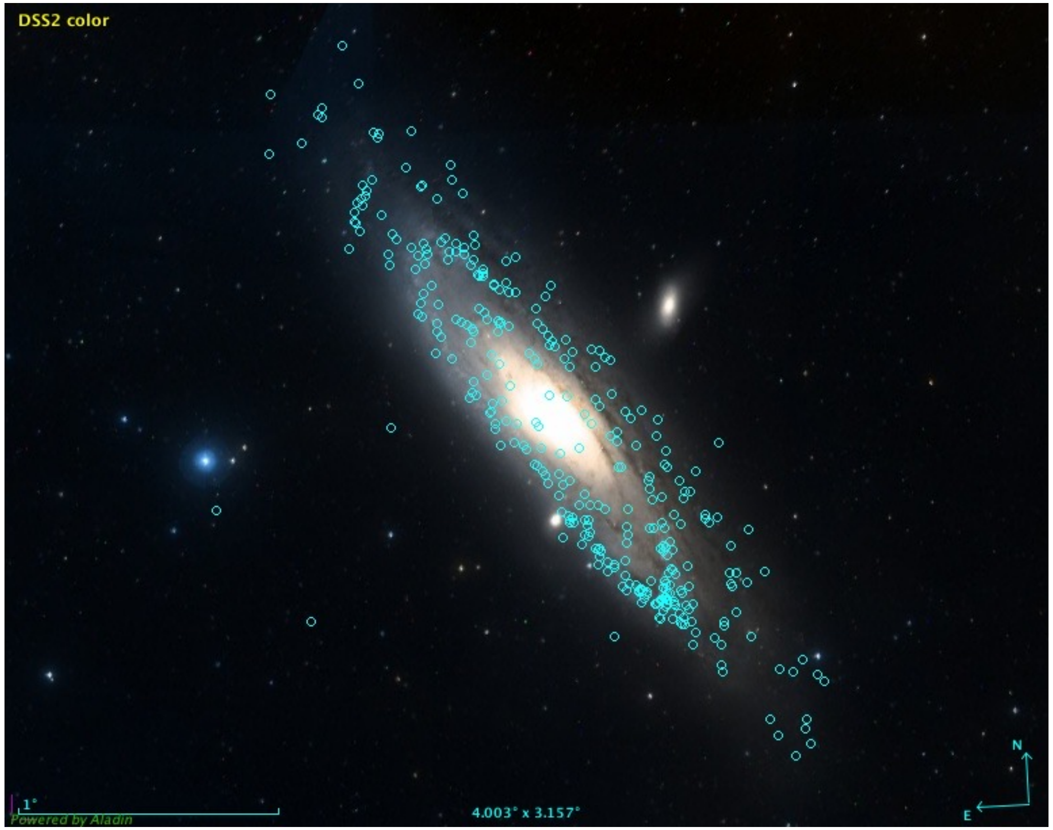

Ripepi et al. 2023

Cepheids in distant galaxies with HST and JWST

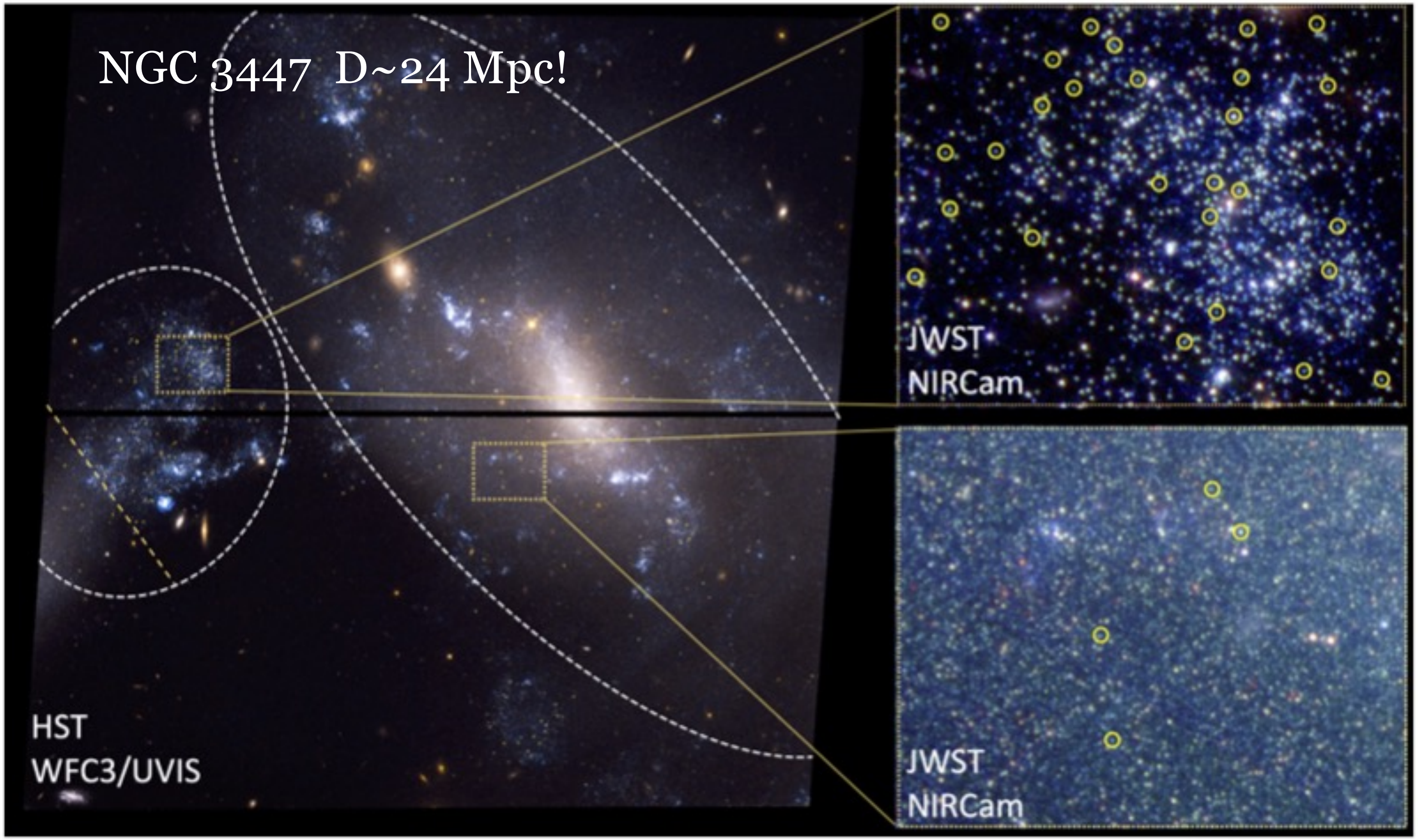

Riess et al. 2025

Variety of Classical Cepheids light-curves

Classical Cepheids can pulsate in different modes. Fundamental, 1rst, 2nd overtones and mixed modes

Fundamental mode have longer periods and larger amplitudes then overtones

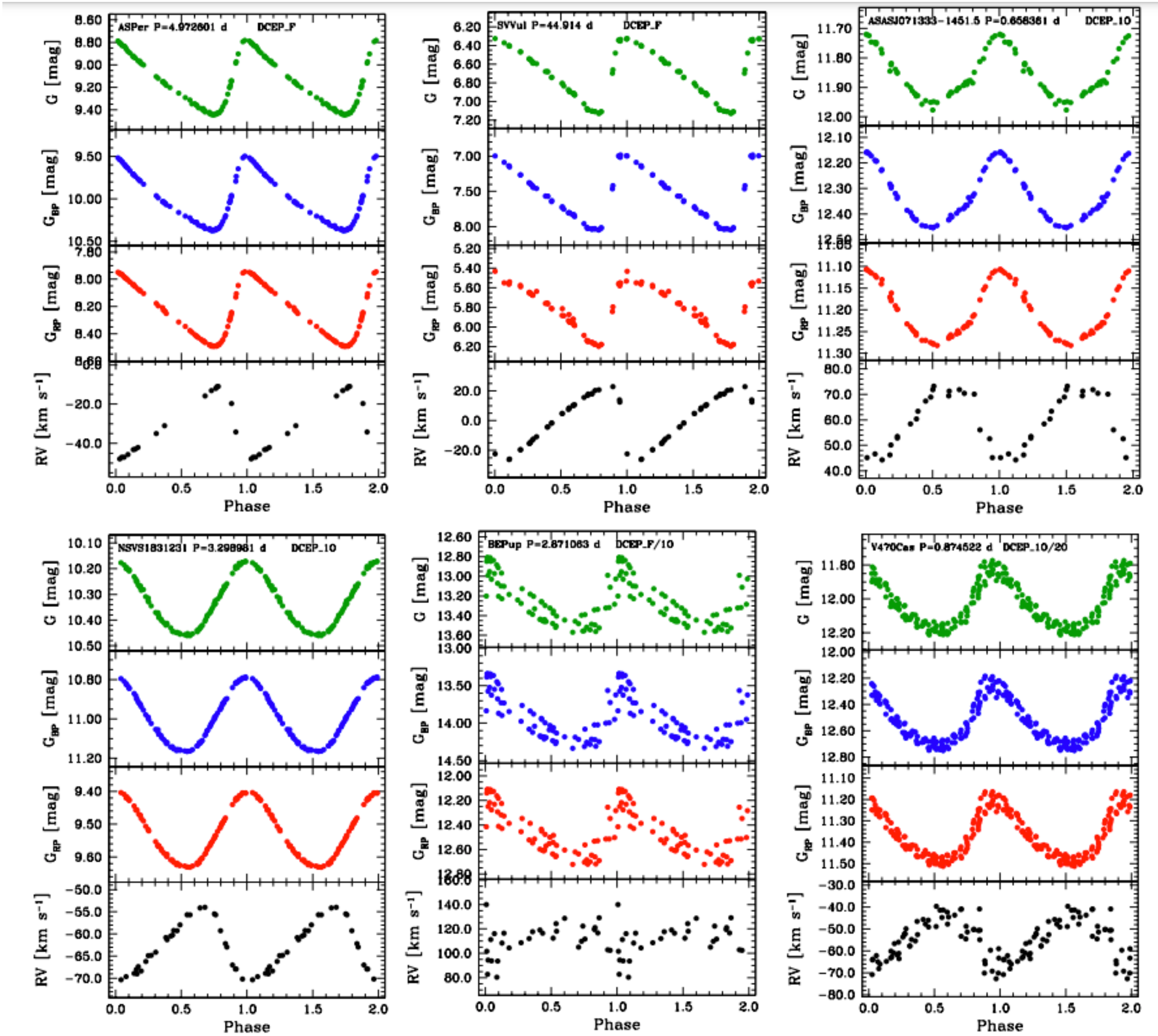

Ripepi et al. 2023

Classical Cepheids: observed CMD

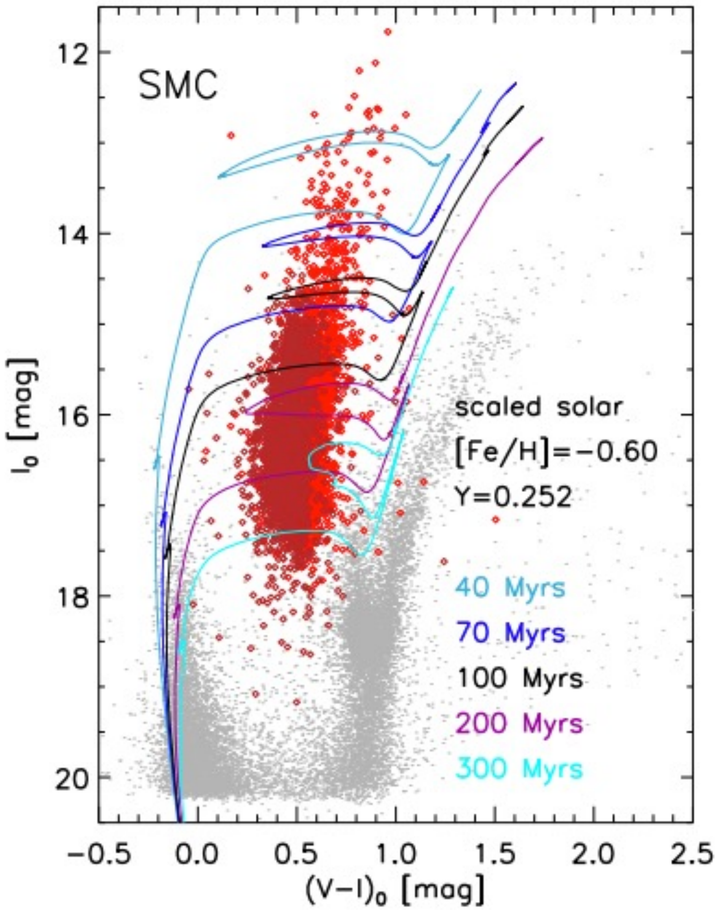

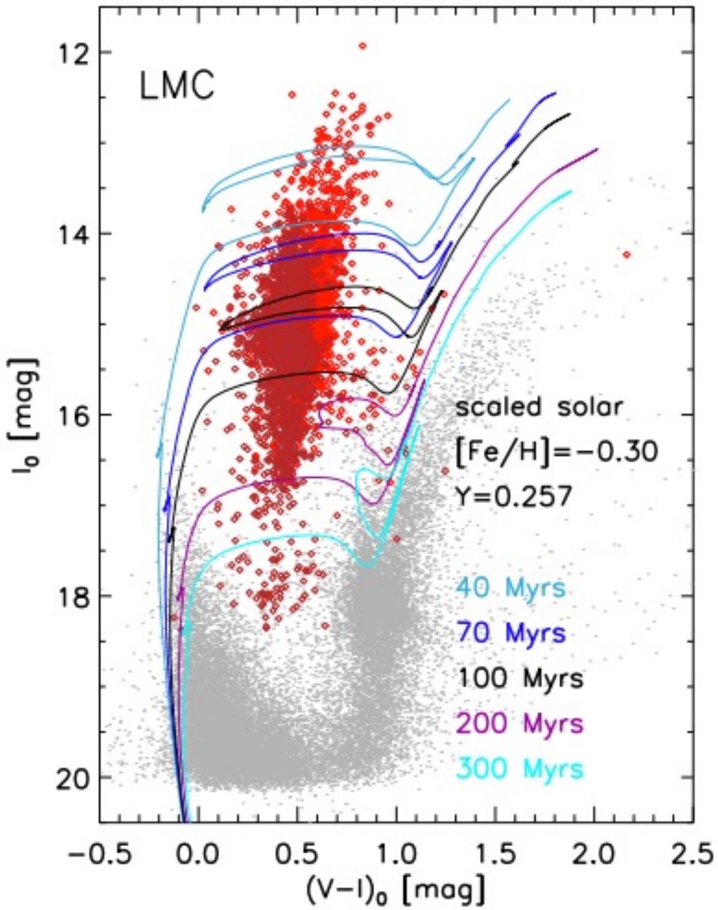

Classical Cepheids are young!

Located in the disc and spiral arms of spiral galaxies and dwarf irregular galaxies rich in gas and young stars (e.g. MW disc, MCs…)

Bono+2024

Type II Cepheids

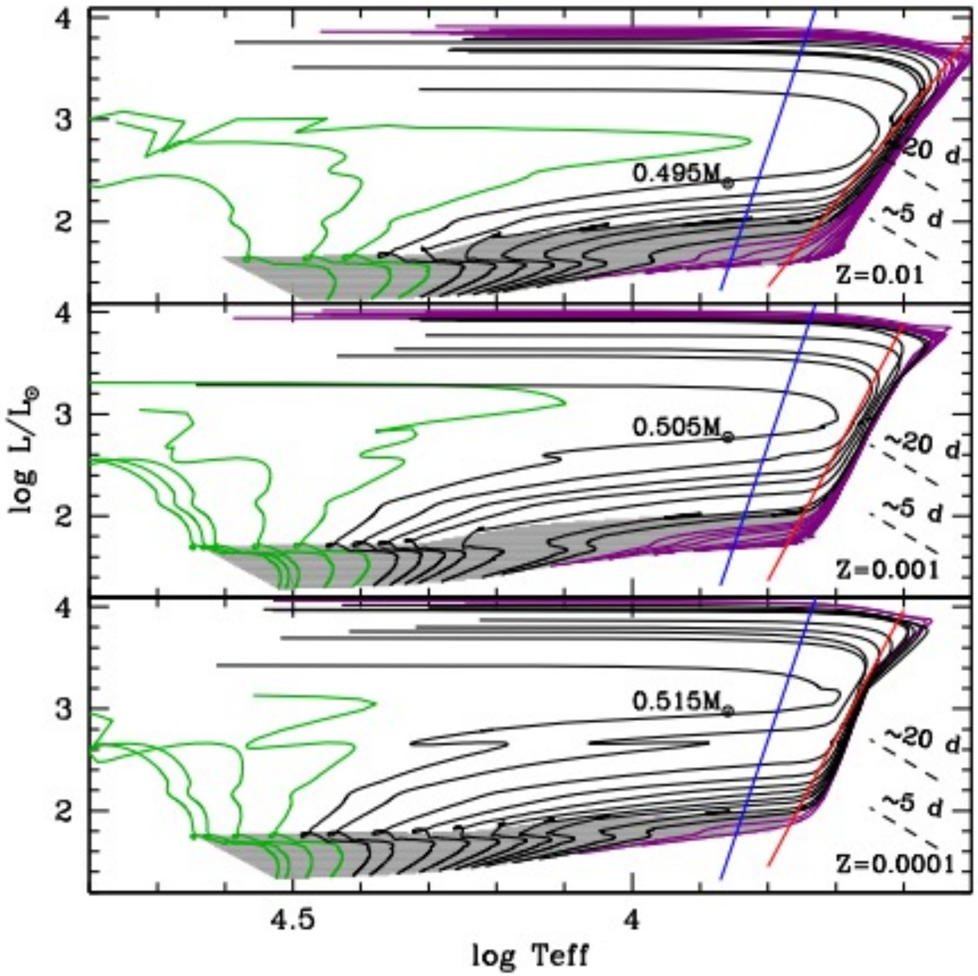

Bono+2020, see also Marconi+2025

BL Her: low-mass evolving from blue HB towards AGB; P~1÷4 d,

W Vir: low mass (post-)AGB stars; He shell flashes P~4÷20 d

RV Tau: low-intermediate mass stars evolving off the AGB. P~20÷100 d

Can be found in the MW, Globular Clusters, MCs

Cepheids in the MW and Magellanic Clouds

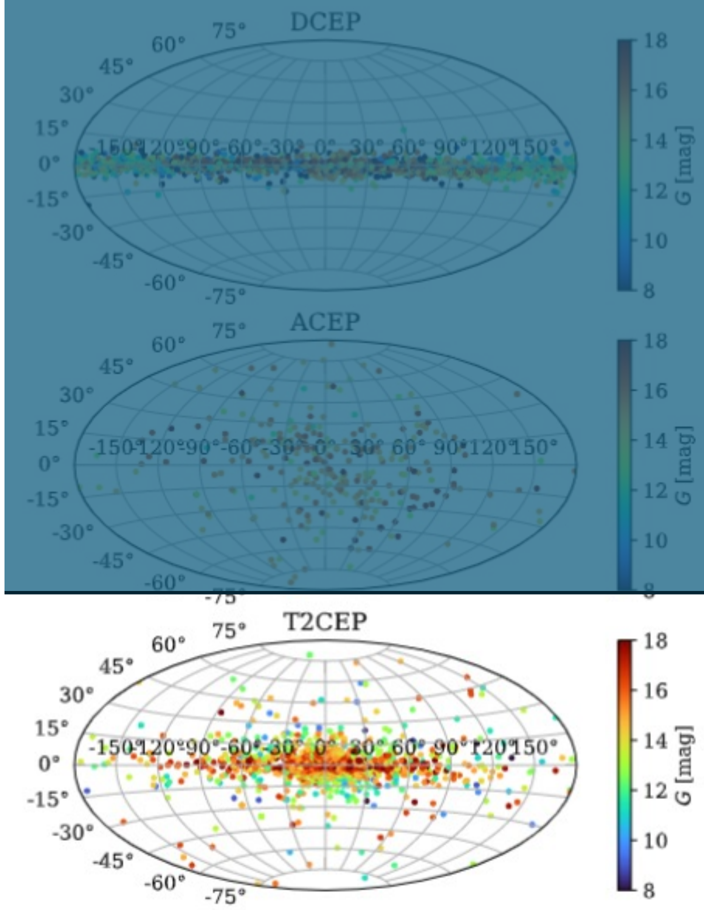

3,434 MW **Classical Cepheids** in Gaia DR3 → largest homogeneous dataset published so far.

~9,000 Cepheids in the Magellanic Clouds

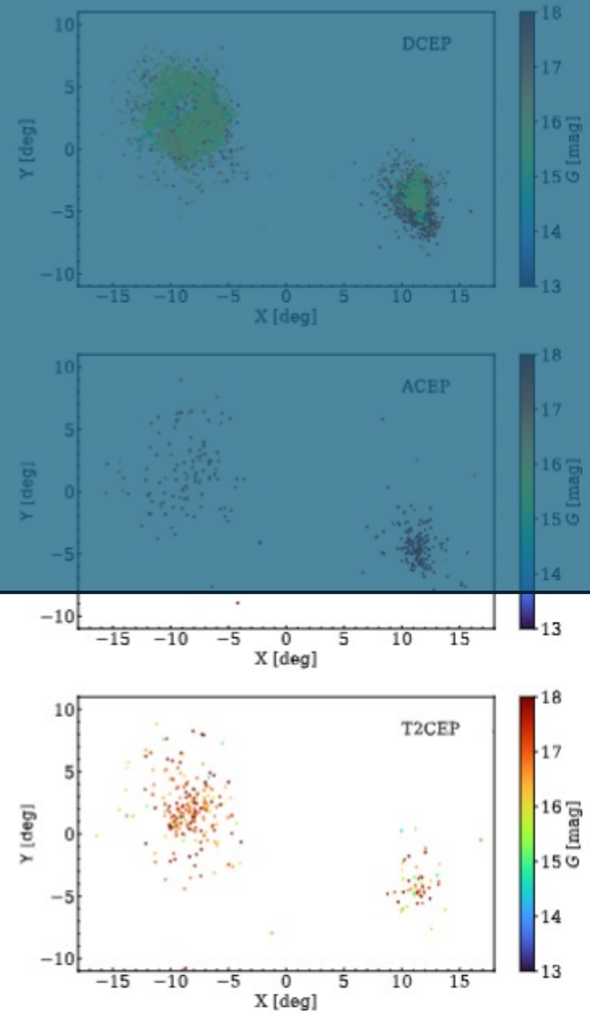

Ripepi et al. 2023

Type II Cepheids: the prototypes

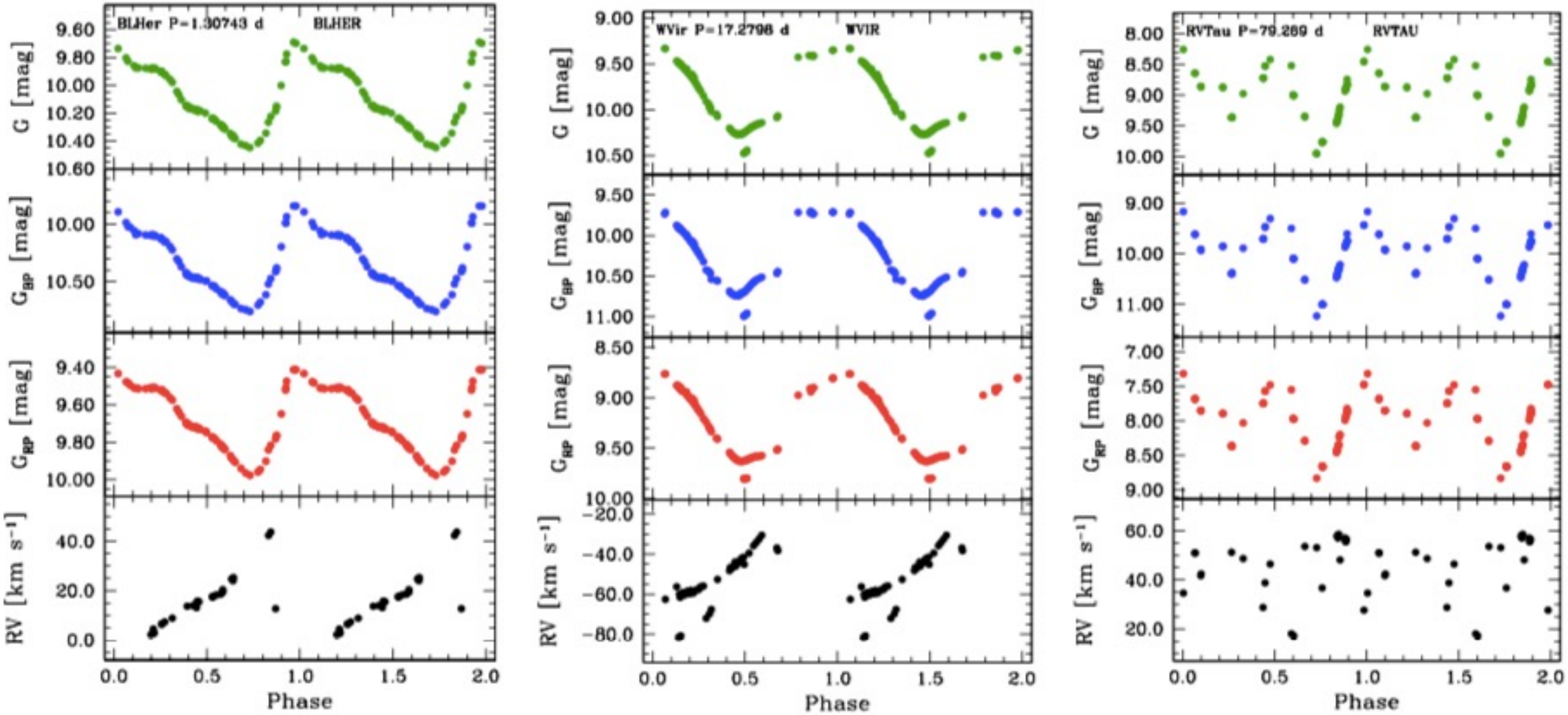

Fig. A.2. Light and RV curves for the prototypes of the BLHER (left), WVIR (centre) and RVTAU (right) classes.

Ripepi et al. 2023

Type II Cepheids: observed CMD

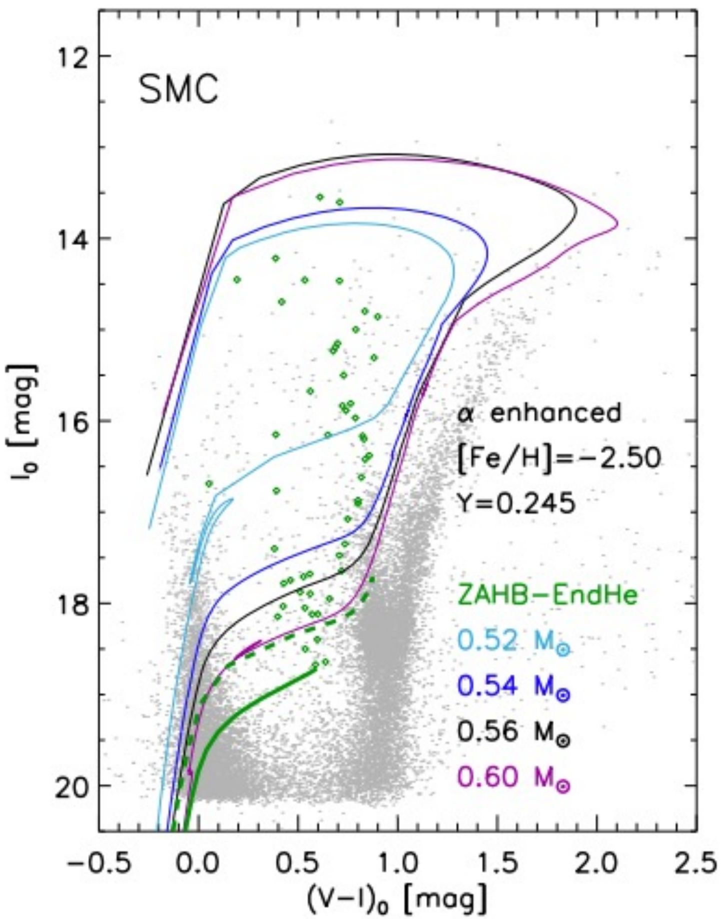

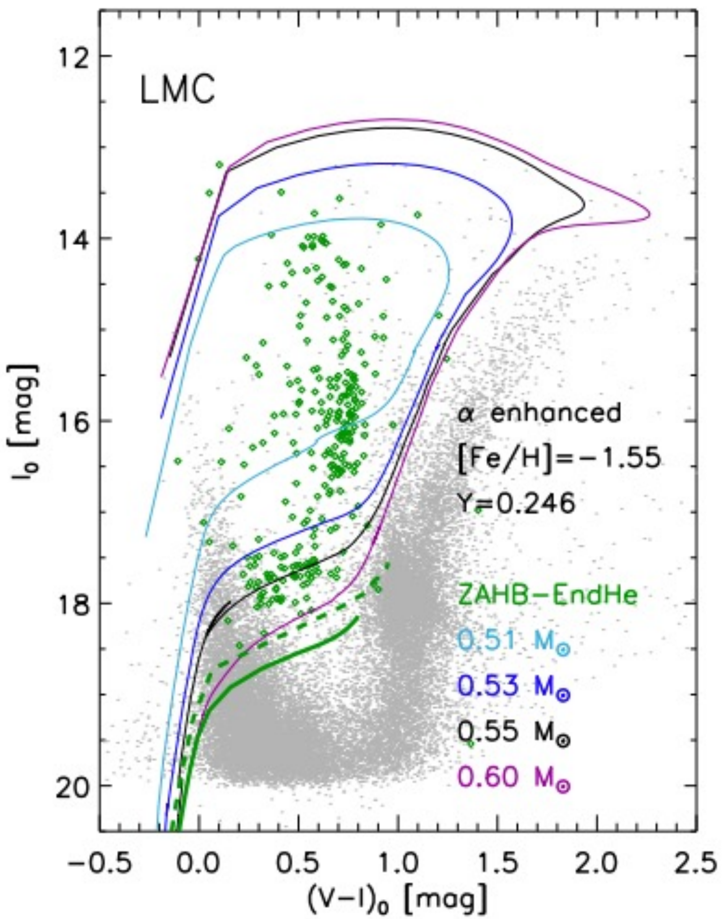

Bono+2020

Type II Cepheids are old objects

Age > 10 Gyrs;
As old as RR Lyrae stars.

Ambiguity only for RV Tau, could be intermediate age stars (few Billion years old).

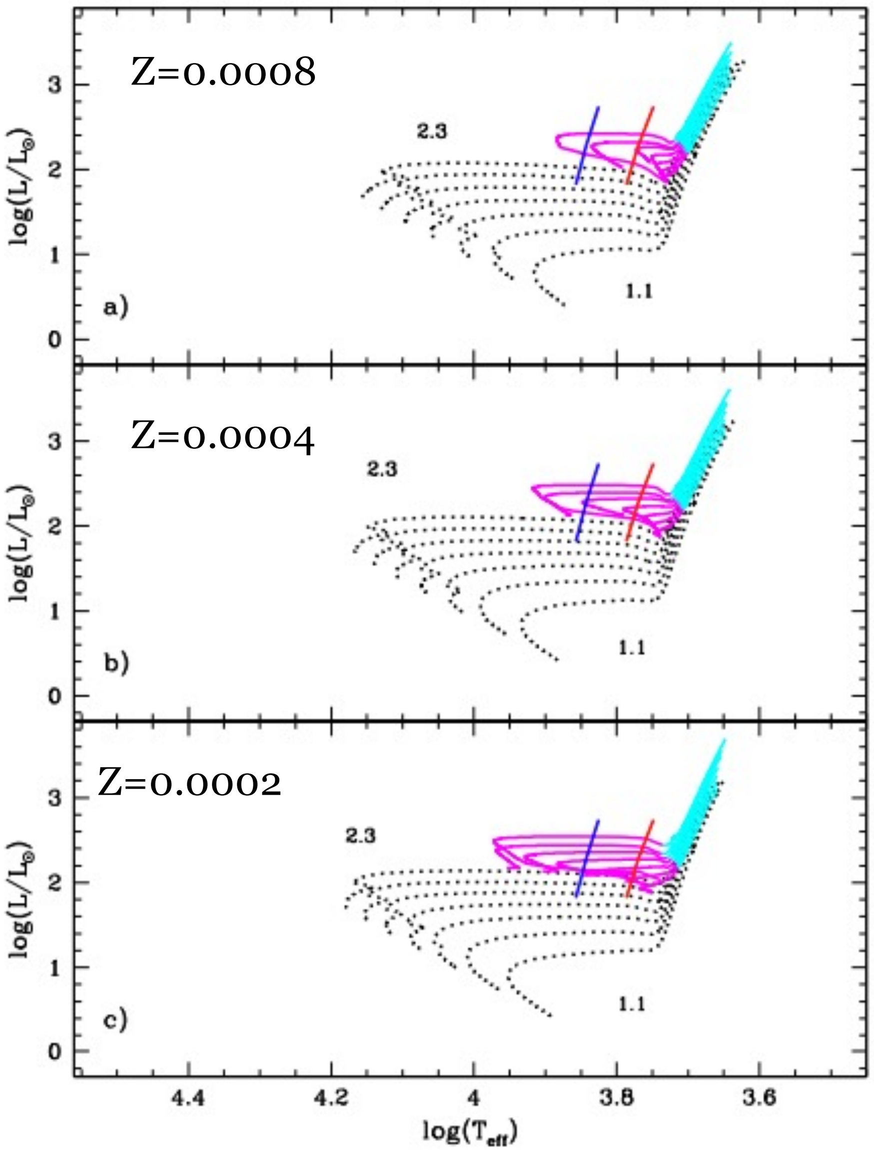

Bono+2024

Anomalous Cepheids

Central helium burning **low metallicity** stars ($M=1.2 \div 2.6 M_\odot$, $M_V=0 \div -2$ mag, $P=0.5 \div 2.5$ d).

Pulsate in F, 1O modes.

Can be found in the MW, MCs, dwarf Spheroidal galaxies (Carina, Sculptor, Fornax….)

Anomalous Cepheids

ACEPs ignite the He in a partially degenerate core.
In the mass range ~1.3–2.3 $M_{\odot}$ (t~1-6 Gyr) stars in their central helium burning cross the classical instability strip at higher luminosities than RRLs only if they are sufficiently metal-poor.

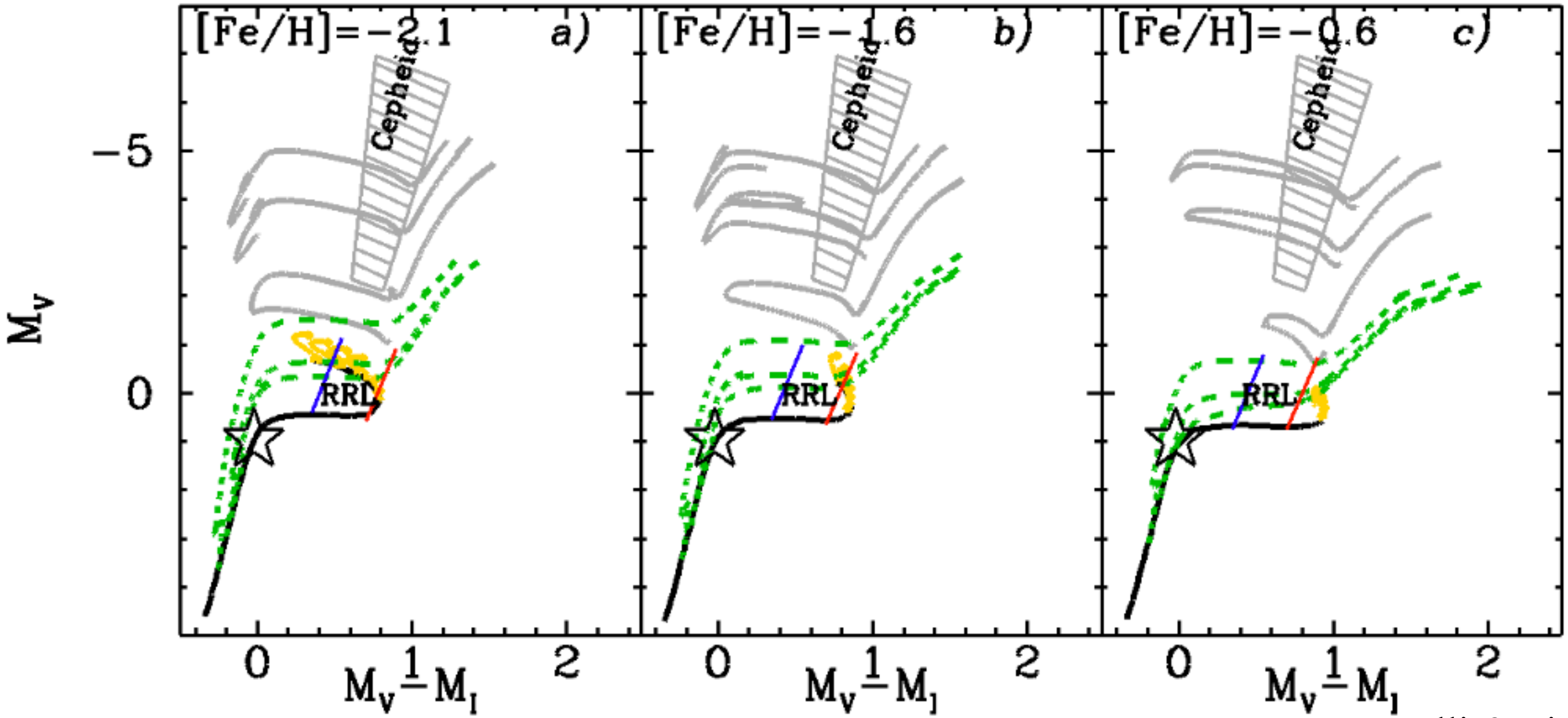

Monelli & Fiorentino 2022

Cepheids in the MW and Magellanic Clouds

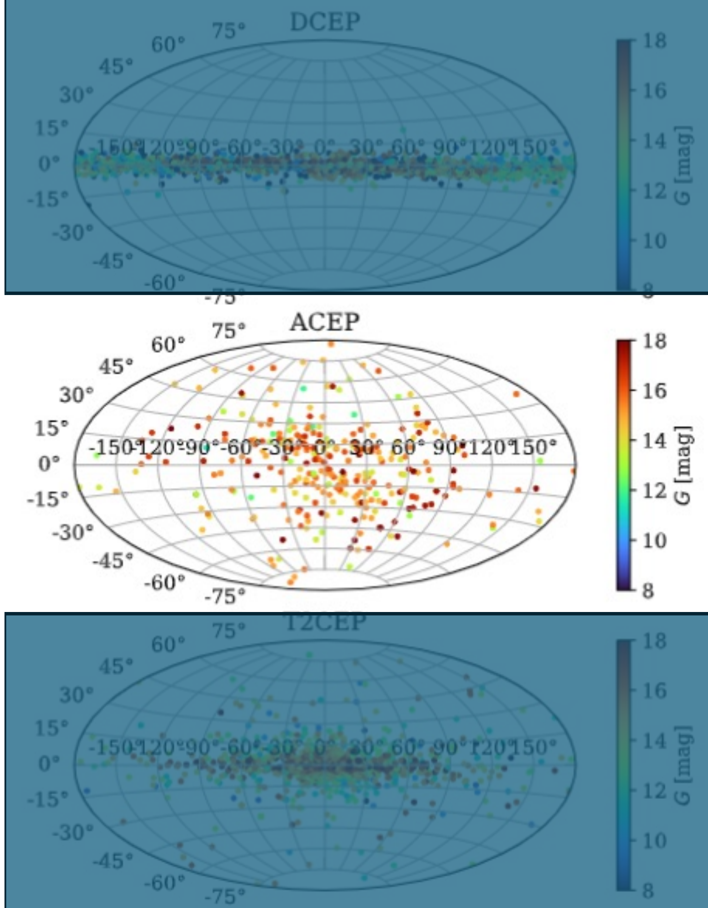

3,434 MW **Classical Cepheids** in Gaia DR3 → largest homogeneous dataset published so far.

Typical of dwarf Spheroidal galaxies

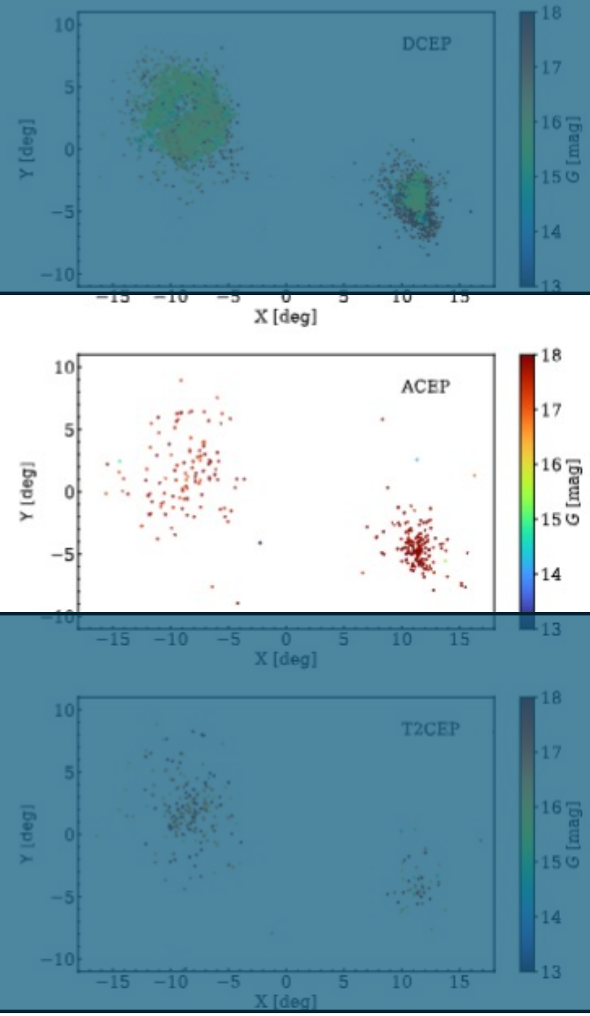

Ripepi et al. 2023

Anomalous Cepheids

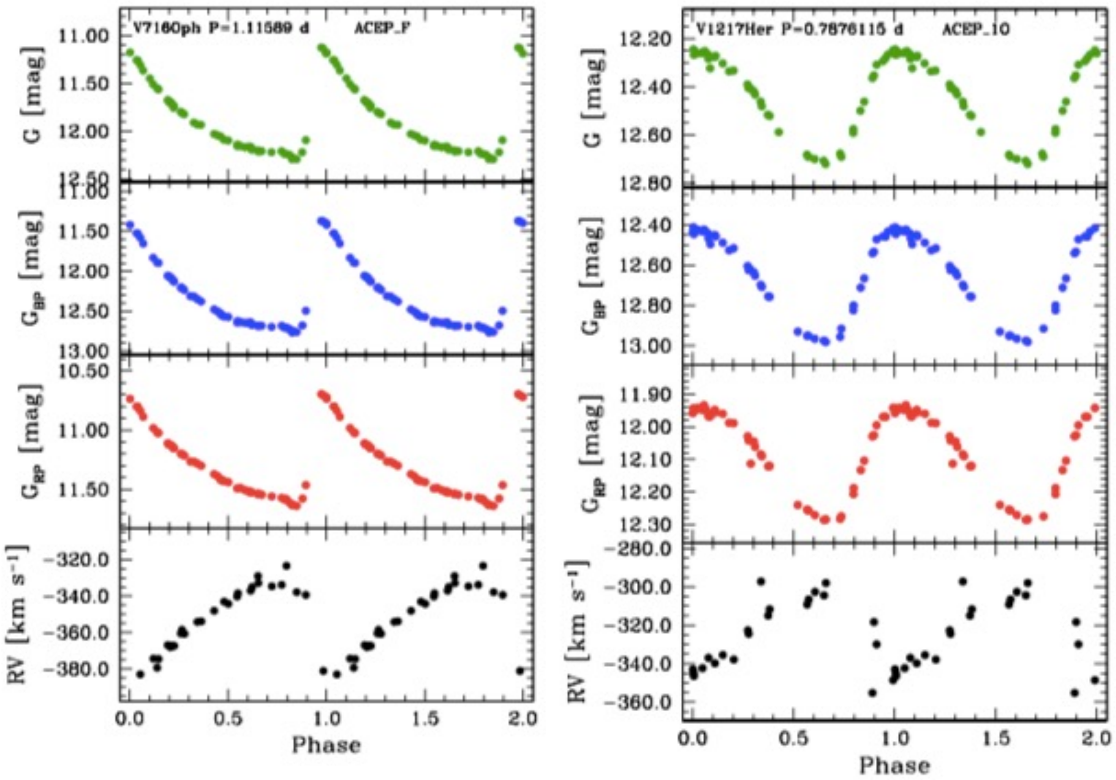

Fig. A.3. Light and RV curves for an ACEP_F (left) and an ACEP_1O (right) variables.

Ripepi et al. 2023

Light curve very similar to RR Lyrae and Classical Cepheids at similar periods →
very difficult to assign the right class without an accurate distance

Anomalous Cepheids in the CMD

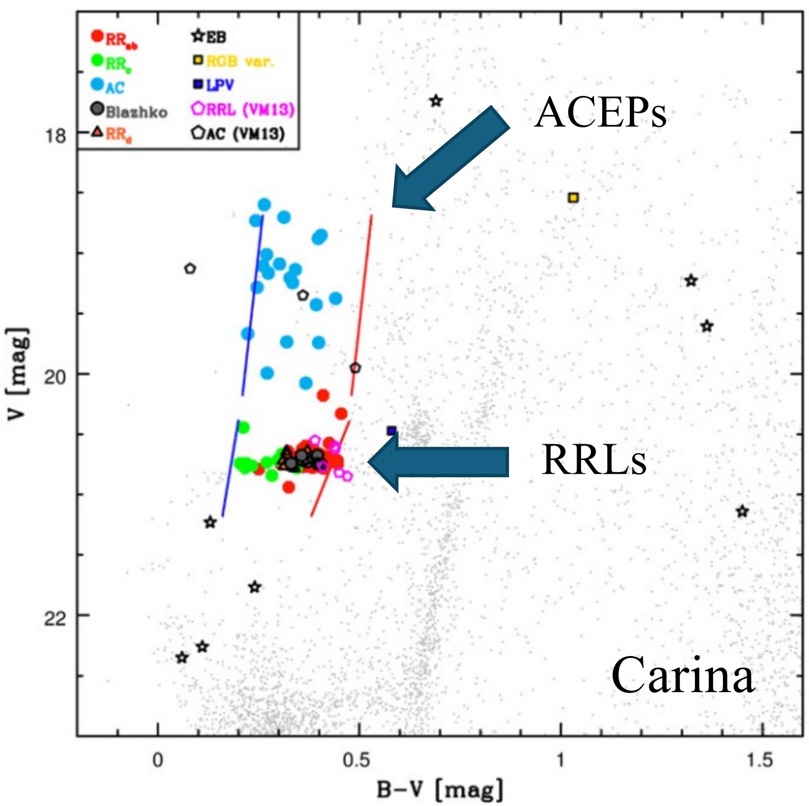

Coppola+2015

Period distribution and CMD location strictly connected to the SFH of the host galaxy.

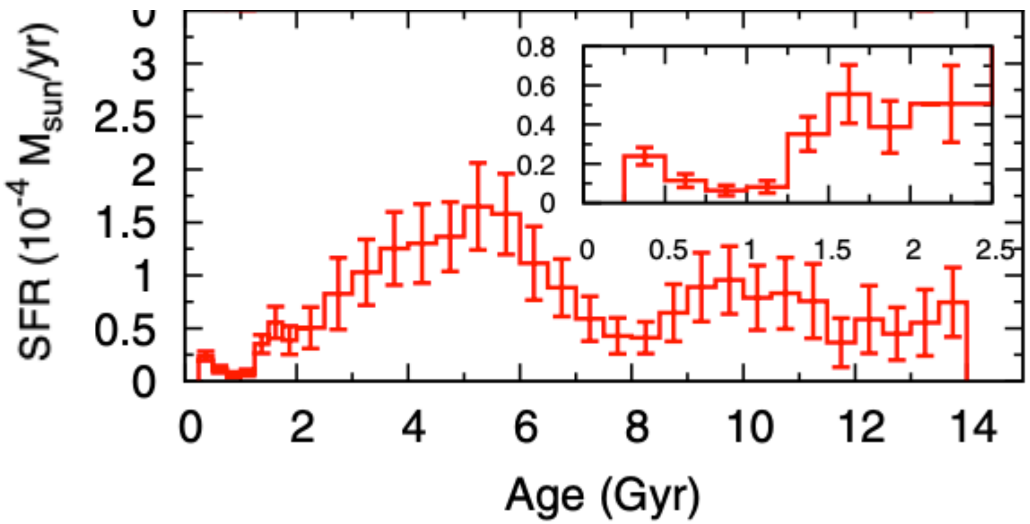

de Boer+2014

Origin of ACEPs

- ~270 ACEPs in the MCs and a total of ~310 additional ACEPs in 37 dwarf galaxies of the LC and other close groups (OGLE IV, Fiorentino & Monelli 2022).
- ACEPs in galaxies with pure old population (t>10 Gyr, e.g. Ursa Minor, Draco, Sextans etc.) and with an extended SFH and a significant intermediate age population (t ~1-6 Gyr, e.g. Carina, Fornax, etc.).
- Only 2 confirmed ACEPs in Galactic GC (i.e. age > 10 Gyr): NGC5466 and M92 – Ngeow+2022
- These evidences suggest two evolutionary channels of formation for the ACEPs (see review by Fiorentino & Monelli, Universe 2022)
    - Single intermediate-age star (e.g. Norris & Zinn 1975)
    - Mass transfer in evolved binaries (e.g. Renzini+1977, Gautschy and Saio 2017 → could also explain ACEPs as metal rich as the LMC)

Common properties of light curves

Classical Cepheids

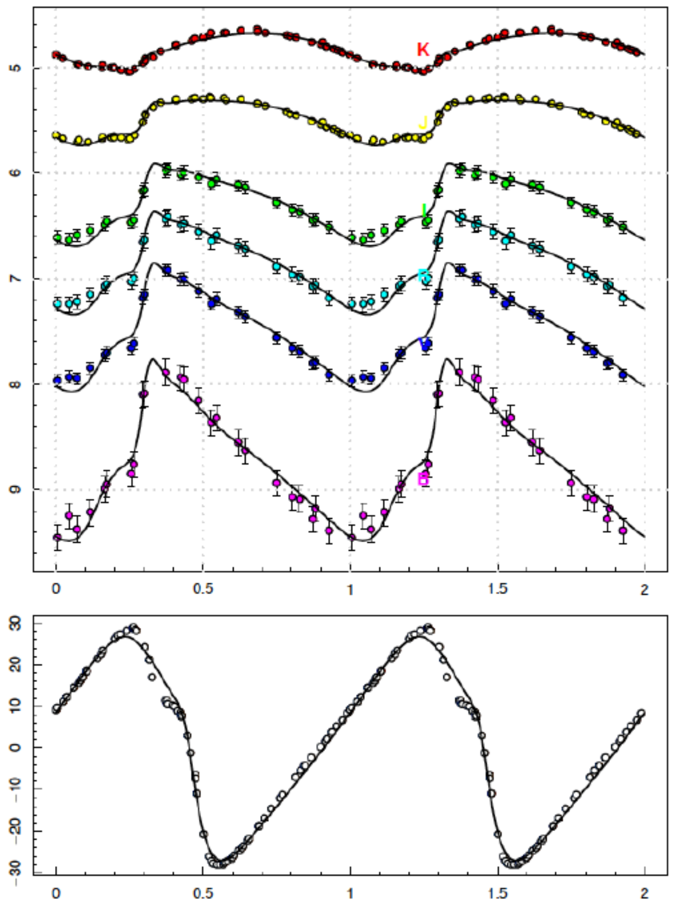

- Light curve amplitude decreases from optical to near infra-red (NIR) wavelength

- $L \sim R^2 T_e^4$ in the optical, while $L \sim R^2 T_e^{1.5}$ in the NIR → in the optical the variation of T_e dominates the pulsation, in the NIR it is the variation of radius that dominates.

- In a typical Cepheid the variation of radius is ~10%, while the T_e can vary by 500-1000 K

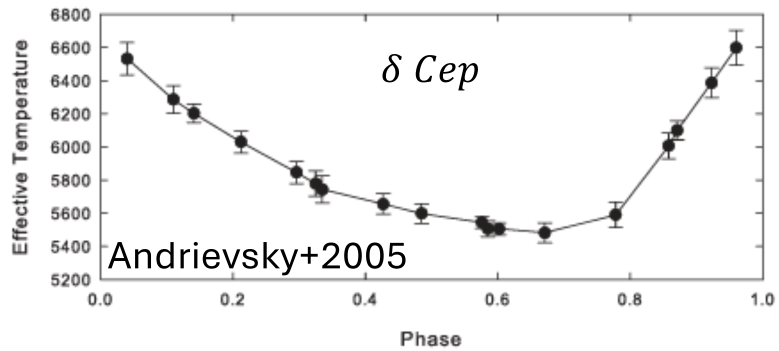

The pulsation cycle

- The maximum brightness of a pulsating star occurs when the least mass between the hydrogen ionisation zone and the star's surface is at a minimum.
- Although the energy beneath the hydrogen ionisation zone peaks when the star's radius is at a minimum, there is some inertia in upper layers: 5-10% of L is temporarily stored in outer layers and released later as this energy propels the hydrogen ionisation zone towards the star's surface.
- The observed luminosity of the pulsating star is thus at a maximum slightly after the star has been compressed to its smallest radius.

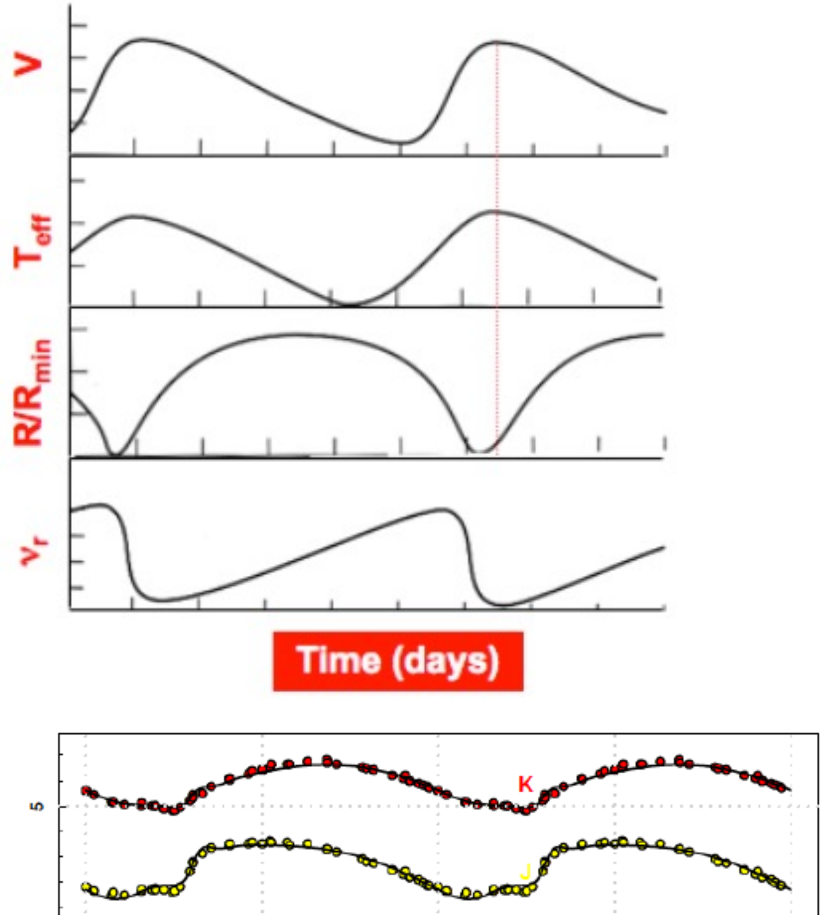

Observational study of the light curves

Main quantities usually measured to characterise and classify pulsating stars:

1. Period(s – for multi-mode stars), and Epochs of maximum light (or radial velocity) – in days

2. Average magnitudes in the different bands (usually the light curves converted in flux, averaged and then converted back in magnitudes)

3. Peak-to-peak amplitudes in the different bands (mag)

4. Fourier Parameters

Period, Amplitude and Fourier parameters in pulsating stars

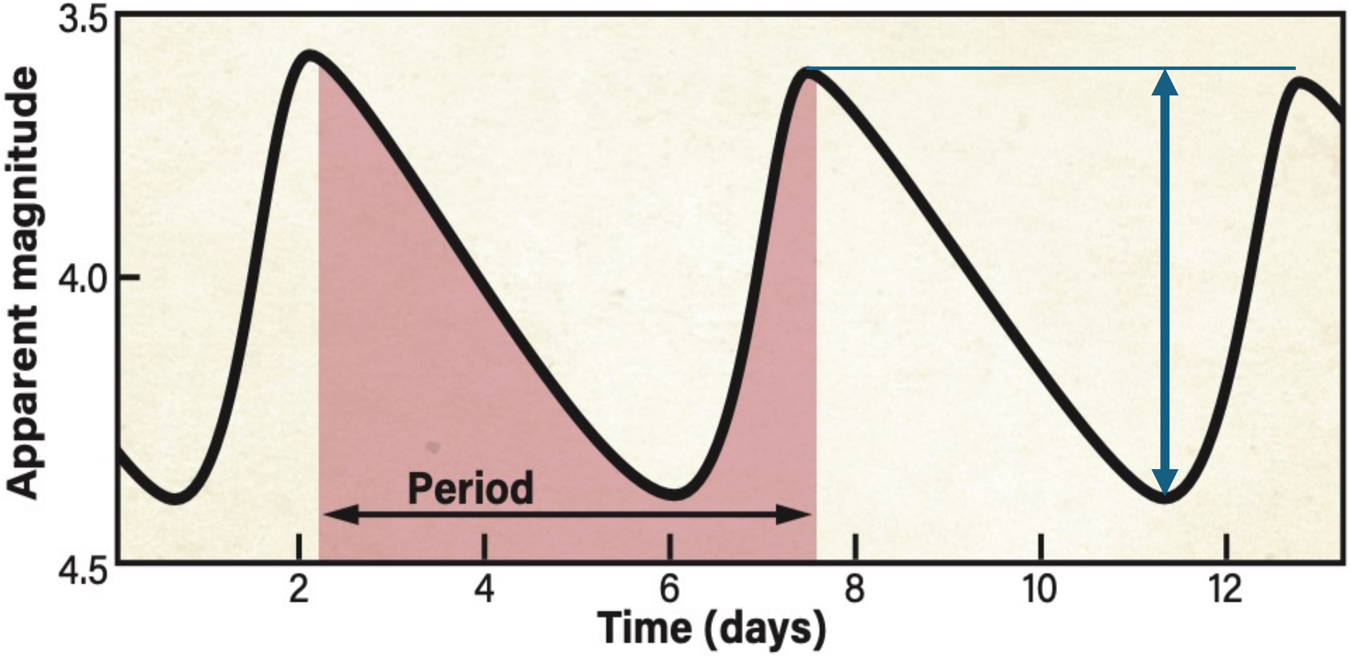

Peak-to-peak amplitude

Credit: Astronomy: Roen Kelly, after R Nave/Hyperphysics

Period, Amplitude and Fourier parameters in Gaia DR3 RR Lyrae and Cepheids

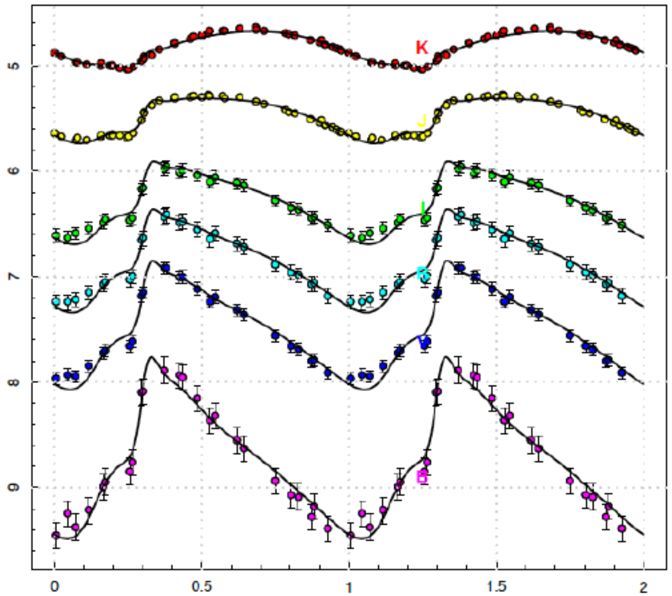

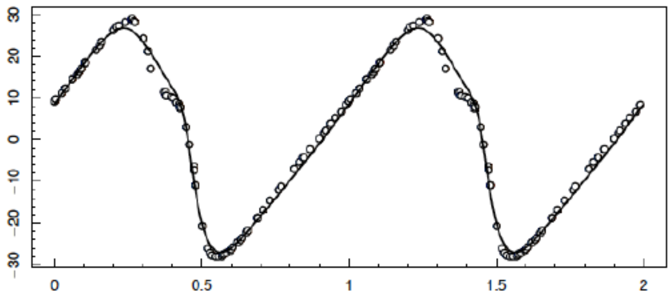

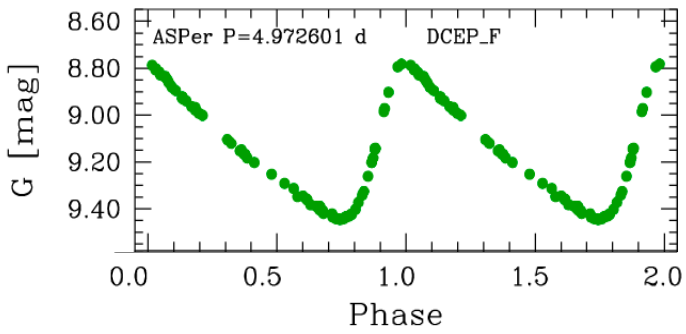

Light curve fitting with Truncated Fourier series

$$\mathrm{mag}(t_j) = zp + \sum [A_i \sin(i \times 2\pi\nu_{\max} t_j + \phi_i)]$$

From the fitted model we derive all the desired quantities:
Intensity averaged magnitudes,
Peak-to-Peak amplitudes.
….

Fourier parameters

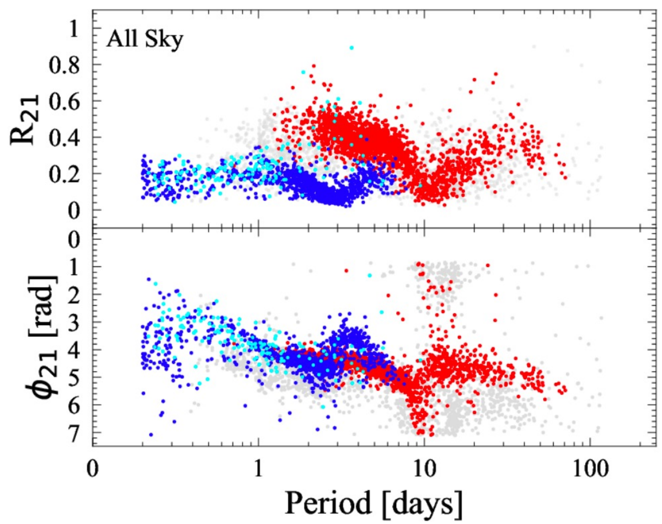

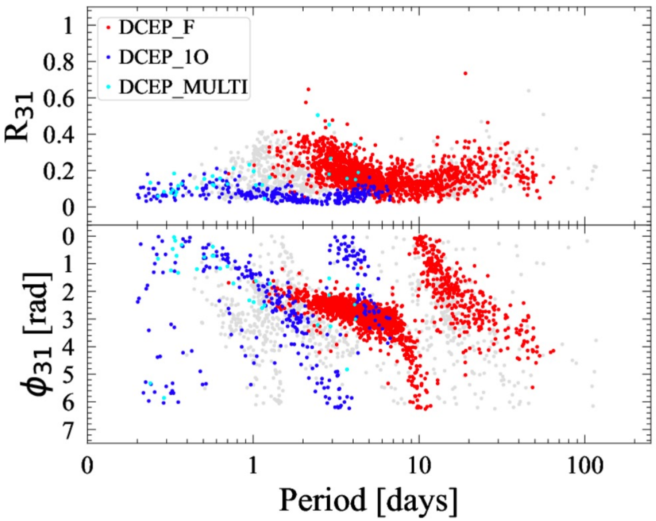

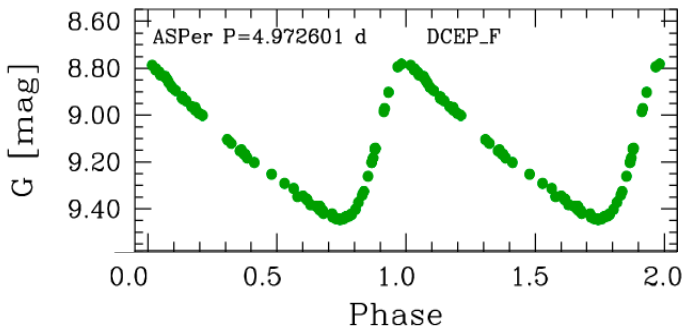

Light curve fitting with Truncated Fourier series

$$\mathrm{mag}(t_j) = zp + \sum [A_i \sin(i \times 2\pi\nu_{\max} t_j + \phi_i)]$$

$$(R_{ij} = A_i/A_j)$$

$$(\phi_{ij} = j \times \phi_i - i \times \phi_j)$$

Ripepi+2023

Period-luminosity relations

Why Cepheids are important? The discovery of the period-luminosity relation

HARVARD COLLEGE OBSERVATORY.

CIRCULAR 173.

PERIODS OF 25 VARIABLE STARS IN THE SMALL MAGELLANIC CLOUD.

The following statement regarding the periods of 25 variable stars in the Small Magellanic Cloud has been prepared by Miss Leavitt.

Leavitt & Pickering (1912)

H. Leavitt

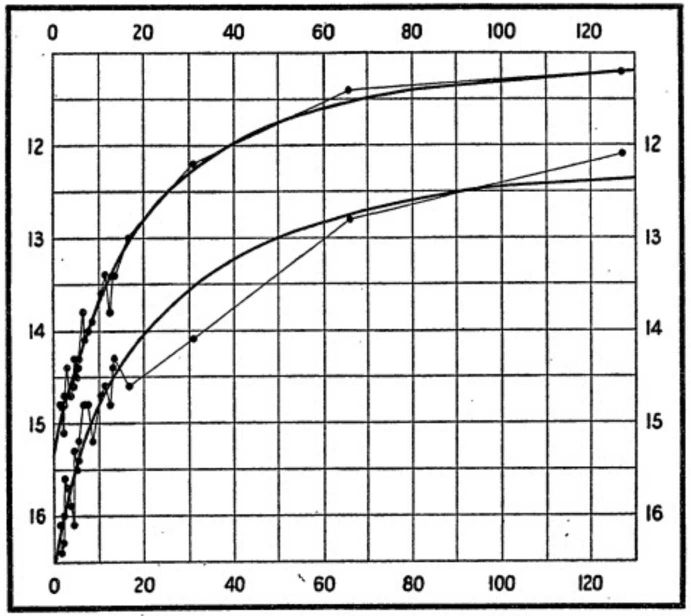

FIG. 1.

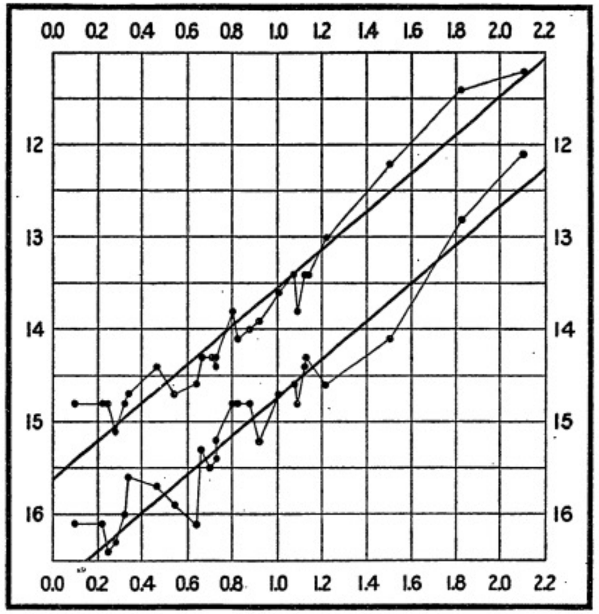

FIG. 2.

1. A straight line can readily be drawn among each of the two series of points corresponding to maxima and minima, thus showing that there is a simple relation between the brightness of the variables and their periods.

Cepheids Period-Luminosity relation

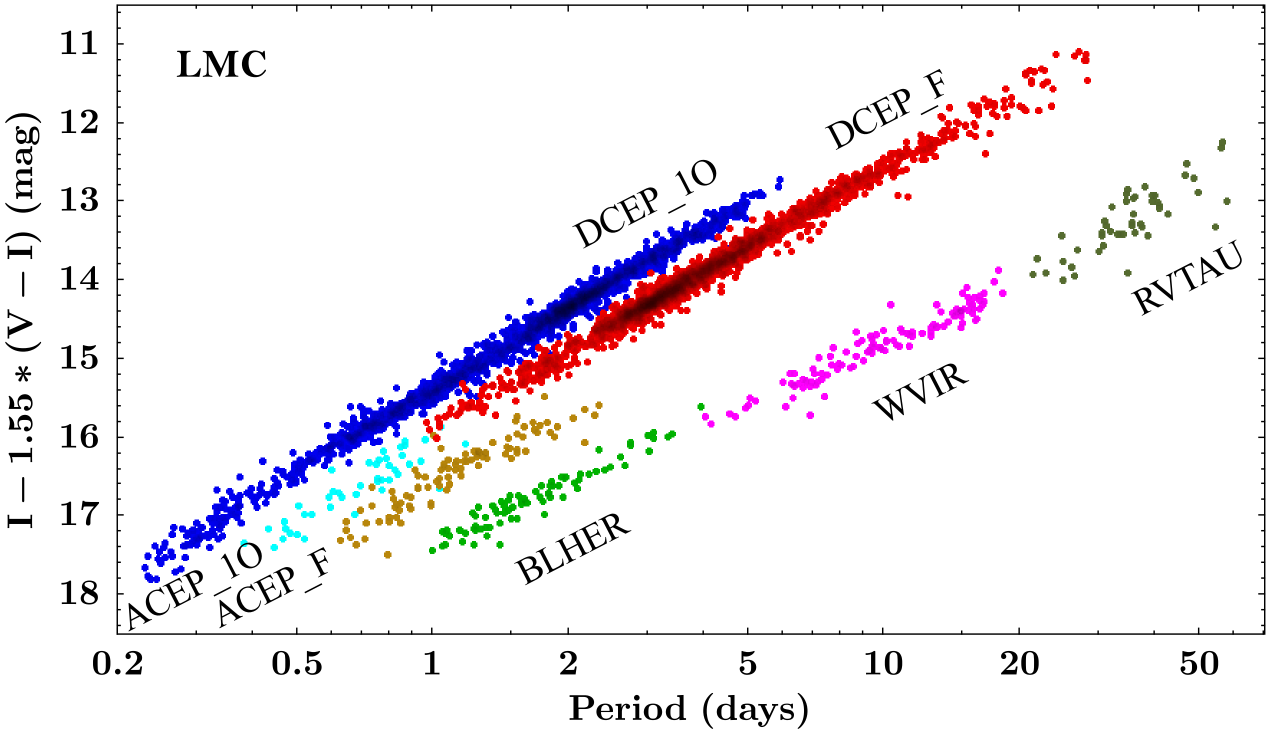

Adapted using OGLE IV data

- All types obey to tight Period-luminosity relations (PLR) → standard candles
- DCEPs → cosmic ladder
- T2CEPs and ACEPs → local group/local volume
- DCEPs are important tracers of the young stellar populations in the host galaxies.

Why is important to study the metallicity dependence of PLRs of DCEPs, T2CEPs and RRLs

All are distance indicators and population tracers of the young (DCEPs) and old populations (T2CEPs and RRLs).

DCEPs → 30-40 Mpc → 100 Mpc with ELT?

T2CEPs → 10 Mpc → 20 Mpc with ELT?

RRLs→ 2 Mpc → 5-7 Mpc with ELT?

Distances and Standard Candles

Distances in astronomy are correlated with the concept of **standard candles** (term introduced by H. Leavitt according to Fernie, 1969)

Standard candles: a class of astrophysical objects which have known luminosity due to some characteristic quality possessed by the entire class of objects. → if an extremely distant object can be identified as a standard candle then the absolute magnitude *M* (luminosity) of that object is known → from the apparent magnitude *m* the distance comes from $m\text{-}M=-5+5log_{10}(D)$.

The characteristics that a good standard candle must have:

Physics-based (i.e., based on a well-understood, theoretically solid physical principle) Examples: Cepheids; Miras (stellar equilibrium equations); Detached binaries, Megamasers (Kepler's law); TRGB (well-understood stellar evolution theory).

Low dispersion of the intrinsic luminosity;

Bright enough and easy to individuate at long distances;

Small observational uncertainties

Control of systematics

Standard Candle for Cepheids: The Period-Luminosity relation. What is its physical origin?

$$\Pi \approx \sqrt{\frac{3\pi}{2\gamma G\rho}}$$

The period-mean density relation also imply that **the period is directly connected with the fundamental stellar parameters, Luminosity (L), effective temperature (Te) and Mass (M).** We can write:

$\Pi \propto \rho^{-1/2}$ *but* $\rho \propto M\, R^{-3}$ $\rightarrow \Pi \propto M^{-1/2}\, R^{3/2}$

Stephan-Boltzman law: $L = 4\pi\sigma\, R^2\, Te^4$ $\rightarrow R \propto L^{-1/2}\, Te^{-2} \rightarrow$

$$\Pi \propto M^{-1/2}\, L^{3/4}\, Te^{-3}$$

i.e. the Period-Luminosity-Color-Mass (PLCM) relation. We shall see that detailed calculation will give exponents of the same order of magnitude. Additional dependence on the abundance in helium and metals (**Y, Z**).

Physical basis of Cepheids' PLC and PL relations

$$\Pi \approx \sqrt{\frac{3\pi}{2\gamma G \rho}} \qquad \Pi \propto M^{-1/2} L^{3/4} Te^{-3}$$

P√ρ= costant → Period is a function of mass, luminosity, effective temperature

Detailed calculations, based on accurate hydrodynamical models allow us to derive for Fundamental mode Cepheids in the Large Magellanic Cloud (Bono, Castellani, Marconi 2000) e.g.:

$$\log_{10} P = 10.557 - 3.28 \log_{10} Te + 0.93 \log_{10} L - 0.79 \log_{10} M$$

Classical Cepheids obey to a Mass-Luminosity-Metallicity relation

$$\log_{10} L = a + b \log_{10} M + c \log_{10} Z + d \log_{10} Y$$

⬇

Period-Luminosity-Color (PLC) relations.

From the PLC to the PL relation

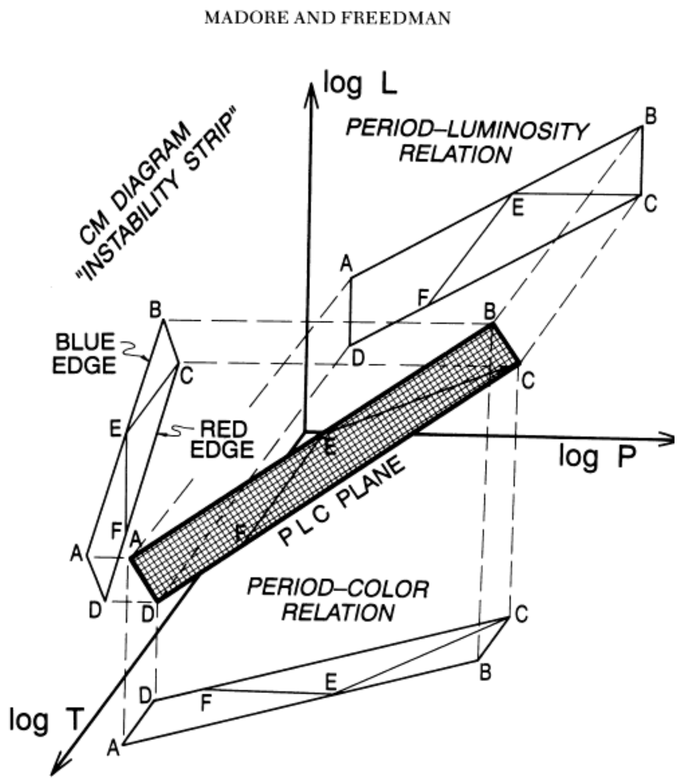

Madore & Freedman (1991)

Observationally, L → $M_{\lambda 1}$; Teff → Color = $M_{\lambda 2}$- $M_{\lambda 1}$ and the PLC relations can be written:

$$M_{\lambda 1} = a + b \times log_{10}P + c \times (M_{\lambda 2} - M_{\lambda 1})$$

The PLC relation holds for each individual Cepheid: measuring the period and the color, one infers the absolute magnitude and in turn the distance.

The PL relation is obtained averaging over the color extension of the instability strip:
It is a statistical relation !! It depends on the number of stars occupying the instability strip and their distribution.

Properties of the PL relations

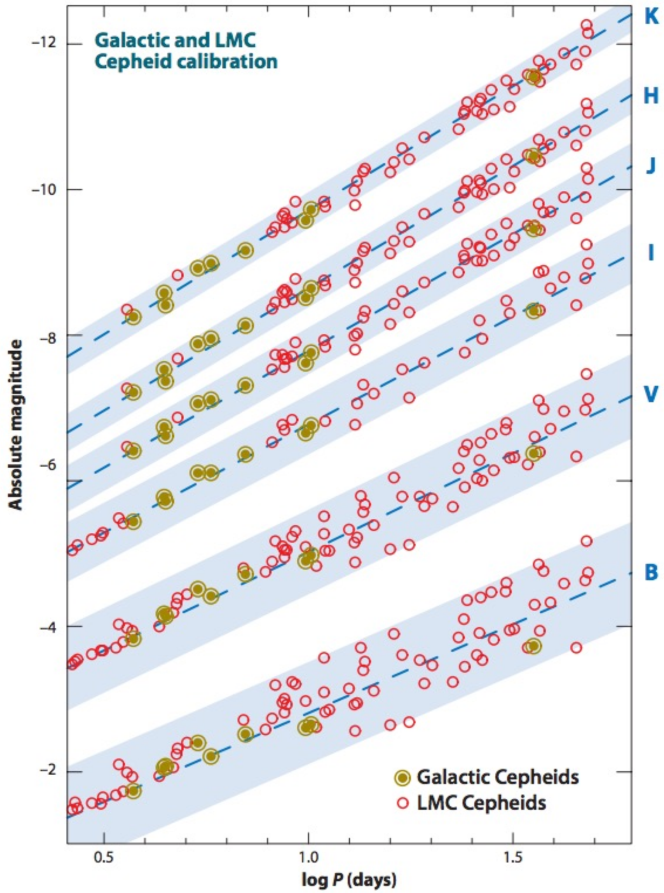

Freedman & Madore (2010)

The slope of the Leavitt Law increases with increasing wavelength, with a corresponding decrease in dispersion.

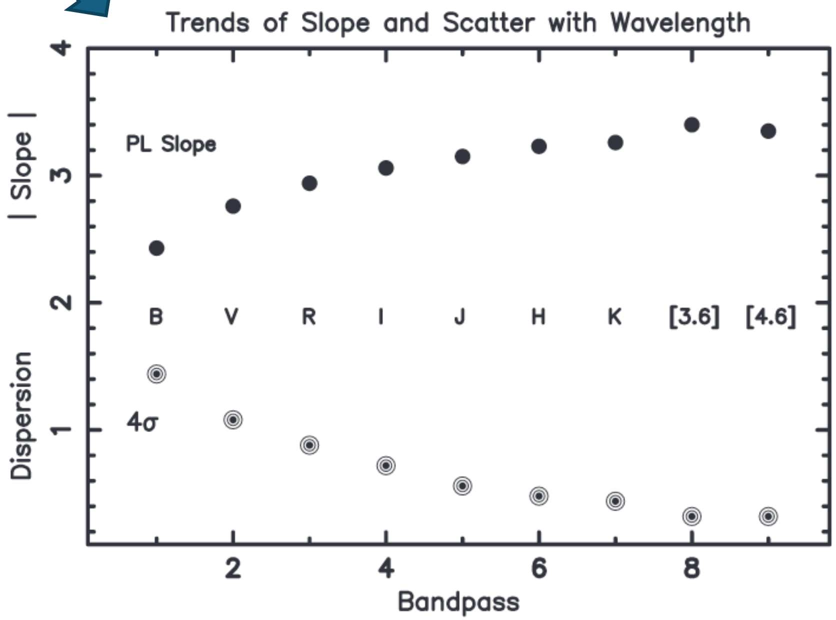

Madore & Freedman (2012)

Properties of the PL relations

The cause is the fact that at longer *wavelenght* λ the instability strip become steeper and narrower.

The physical explanation of this is the different dependence of the surface brightness from Te at different λ.

Rewriting the Stephan-Boltzman law as: $M_\lambda = -2.5 \log R^2 - 2.5 \times a_\lambda \log T_e + b_\lambda,$

Surface brightness

And parametrizing R and Te as: $log\, R = c\, log\, P + d$ $\quad log\, Te = -e\, log\, P + f$

$$M_\lambda^{\rm red} = [-5c + 2.5 e a_\lambda] \log P - 2.5 \times [a_\lambda \times f_{\rm red}] + b_\lambda - 5d \quad (2a)$$

$$M_\lambda^{\rm blue} = [-5c + 2.5 e a_\lambda] \log P - 2.5 \times [a_\lambda \times f_{\rm blue}] + b_\lambda - 5d. \quad (2b)$$

Madore & Freedman (2012)

Properties of the PL relations

$$|M_\lambda| = 2.5 \times a_\lambda |f_{\rm blue} - f_{\rm red}|.$$ → ~ width of the PL

$$\Delta M_\lambda / \Delta \log P = A_\lambda = -5c + 2.5 e a_\lambda .$$ → ~slope of the PL (c ~ 0.7 and e ~ 0.08)

$a_\lambda = 4$ in the optical

$a_\lambda \sim 1.5$ in the K band

→ Explains the observed behaviour of Slope and dispersion of the PL.

Madore & Freedman (2012)

Synthetic multiband PL relations

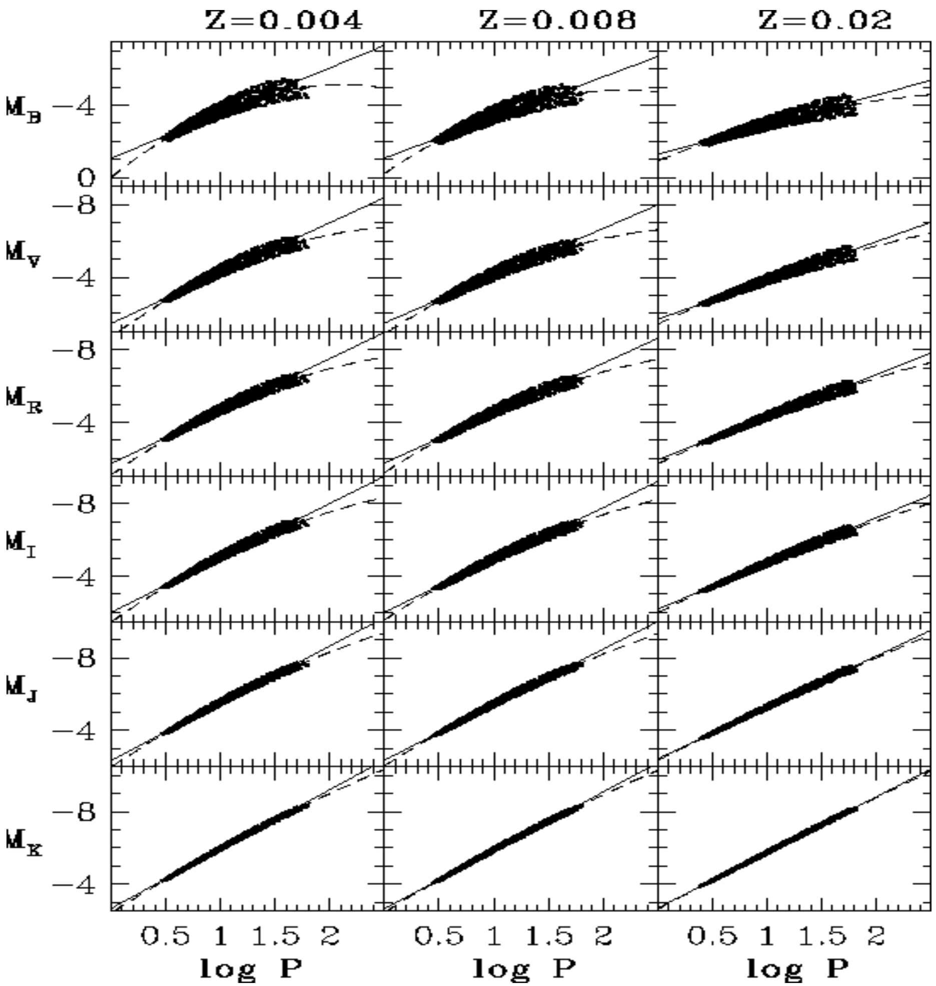

By populating with a mass law distribution the predicted instability strip at varying metallicity it is found that:

Optical synthetic PL depend on metallicity, appear to obey to a non-linear (quadratic) rather than to a linear relation and have a significant dispersion;

All these effect are reduced when we move toward NIR bands.

Caputo et al. 2000 A&A

Properties of the PL relations

PL relations can show breaks in the linearity. Examples in the LMC (First overtones, Ripepi et al. 2022) and SMC (Fundamental, Ripepi et al. 2017).

In the LMC, the cause is likely that Cepheids with P<0.58 d are at their **first crossing of the instability strip.**

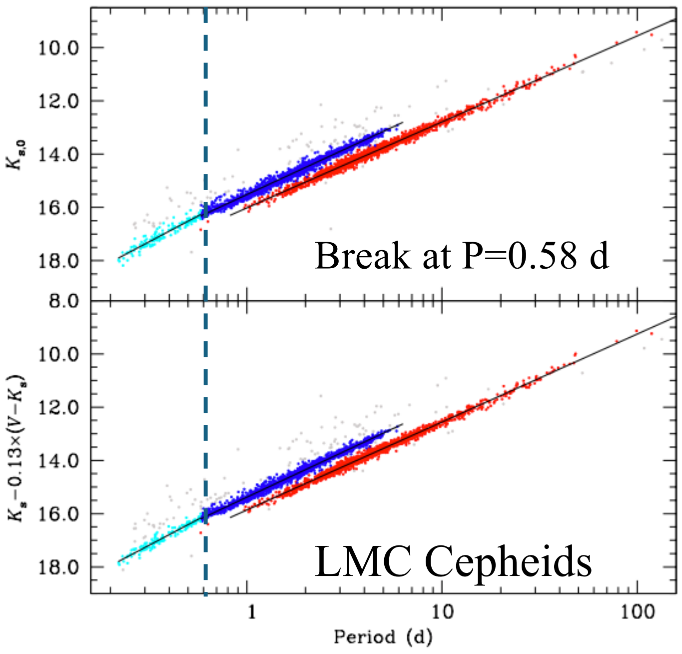

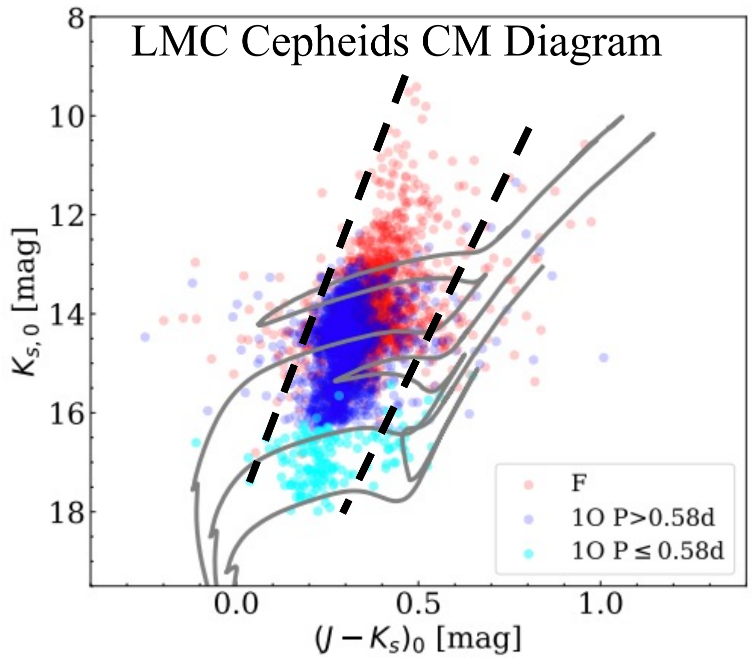

Ripepi et al. 2022

The Wesenheit magnitudes

Why we don't use PLC relations? → High sensitivity to reddening!

Cepheids are usually located in the disc of spiral galaxies, where the presence of gas and dust produce a significant amount of extinction which is not easy to measure, especially in distant galaxies.

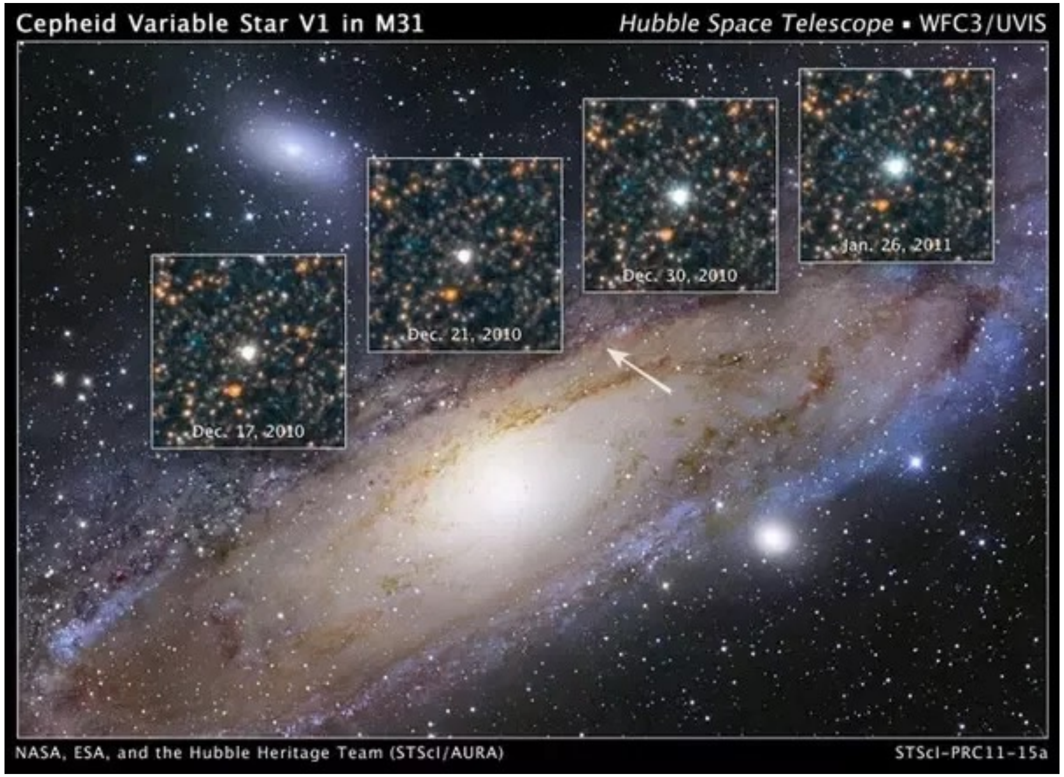

The Wesenheit magnitudes

To bypass the reddening problem, in 1982 B. Madore introduced the so-called Wesenheit magnitudes W (Wesenheit is a German word meaning "essence", "real nature".

We adopt the V,I band as an example (any combination of magnitudes/colors can be used).

In this case, the ratio of total-to-selective absorption is $R_{VI} = A_V / E(V - I)$,

$$\boxed{W = V - R_{VI} \times (V - I),} \tag{10}$$

as well as an intrinsic Wesenheit magnitude, W_o:

$$W_o = V_o - R_{VI} \times (V - I)_o. \tag{11}$$

By construction,

$$W = V_o + A_V - R_{VI} \times (V - I)_o - R_{VI} \times E(V - I) \tag{12}$$

$$= V_o - R_{VI}(V - I)_o + A_V - R_{VI} \times E(V - I), \tag{13}$$

where $V = V_o + A_V$ and $(V - I) = (V - I)_o + E(V - I)$, and $A_V = R_{VI} \times E(V - I)$, thereby reducing the last two terms to zero, leaving $W = V_o - R_{VI} \times (V - I)_o$, which is equivalent to the definition of W_o.

Wesenheit magnitudes are reddening free ! → huge reduction of the uncertainty on the measure of H_0

The Wesenheit magnitudes

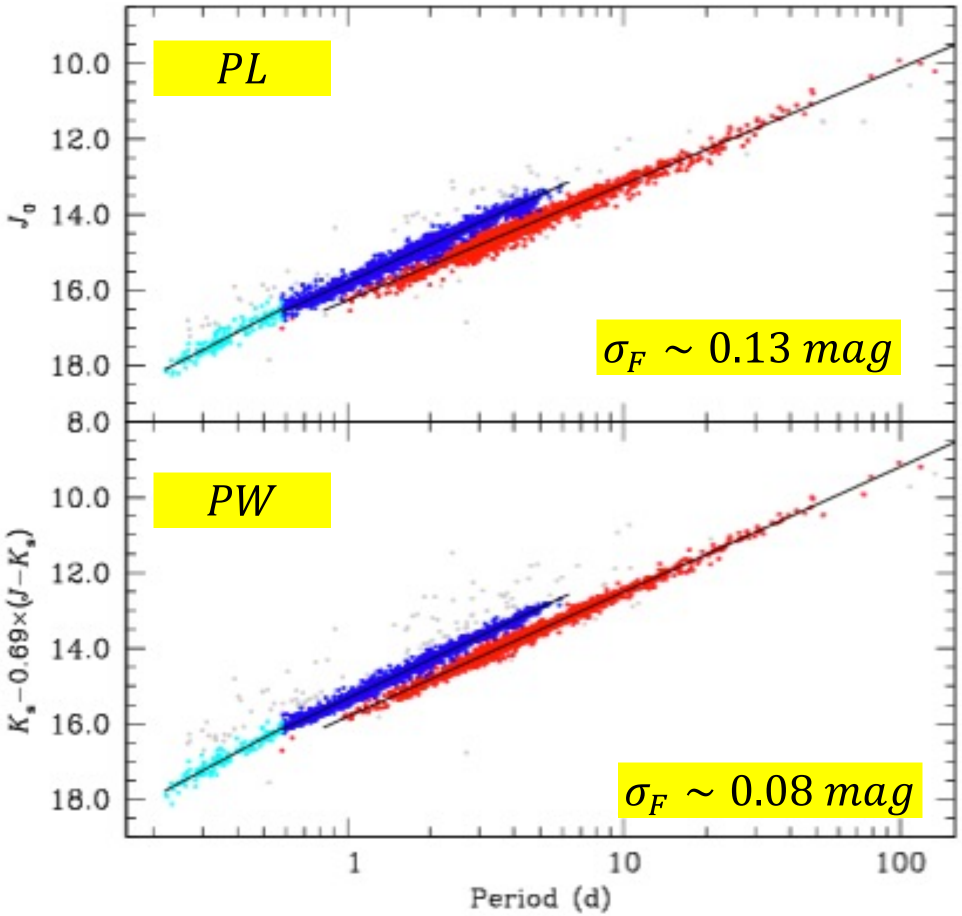

Ripepi et al. 2022

The Wesenheit magnitudes: pro and cons

Pro:

- Low sensitivity to reddening → no need for individual reddening estimations

- PW relations have much smaller dispersion compared to PLs:
  1. The Wesenheit magnitude takes into account the color information → the PW relations are also pseudo PLC relations (Bono et al. 1999) → more accurate location of the individual Cepheids inside the instability strip.
  2. Insensitive to the errors on the individual reddening estimations used to build PL relations.

Cons:

- Sensitivity to the reddening law (Rv, affected by the different dust grain size) which is accurately measured in the MW and then assumed as universal.
  Problem mitigated when using colours mixing opt-NIR bands → the coefficient multiplying the colour is small, almost insensitive in changes of Rv. Example: W(V,Ks)=Ks-0.13*(V-Ks)

RR Lyrae Mv-[Fe/H] and PL Relations in the infrared

PL-relation for RR Lyrae? Not in all bands!

M_V-[Fe/H] relation

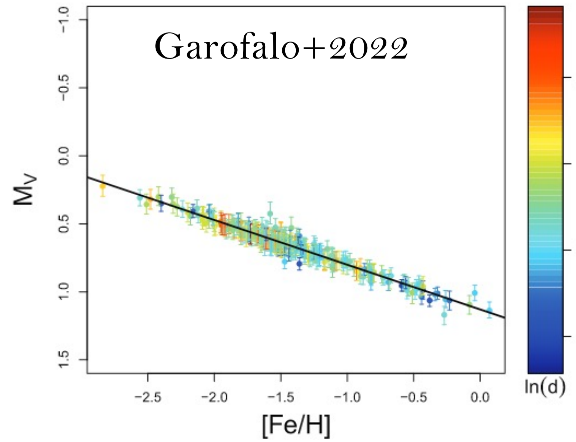

M_K-logP-[Fe/H] relation

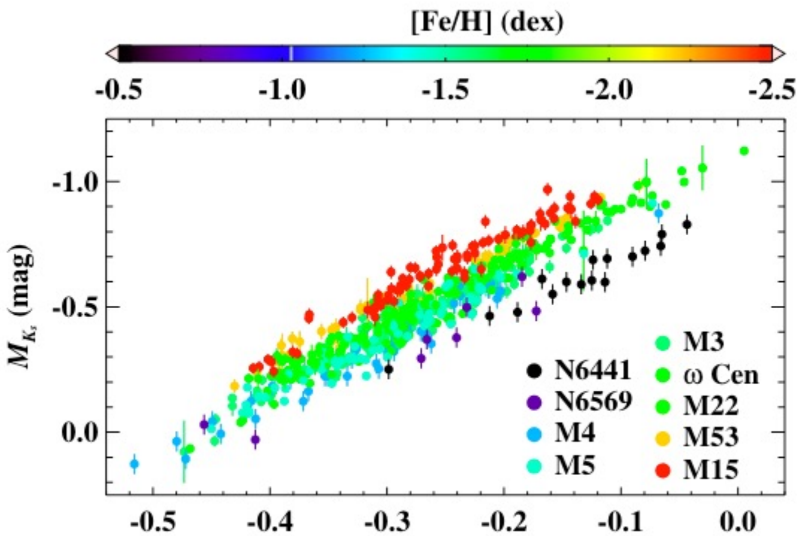

Bhardwaj+2022

No mass-luminosity relation for RR Lyrae variables! The luminosity is fixed by the mass of the He core in the HB phase

The M_V-[Fe/H] relation originates from the fact that if Z increases, the Helium flash happens earlier and the mass of the core at ZAHB is smaller, hance less luminous. At the Te of RRL, $M_{bol} \sim M_V$

M_K-logP-[Fe/H] relation → due to BCs

HB synthetic models

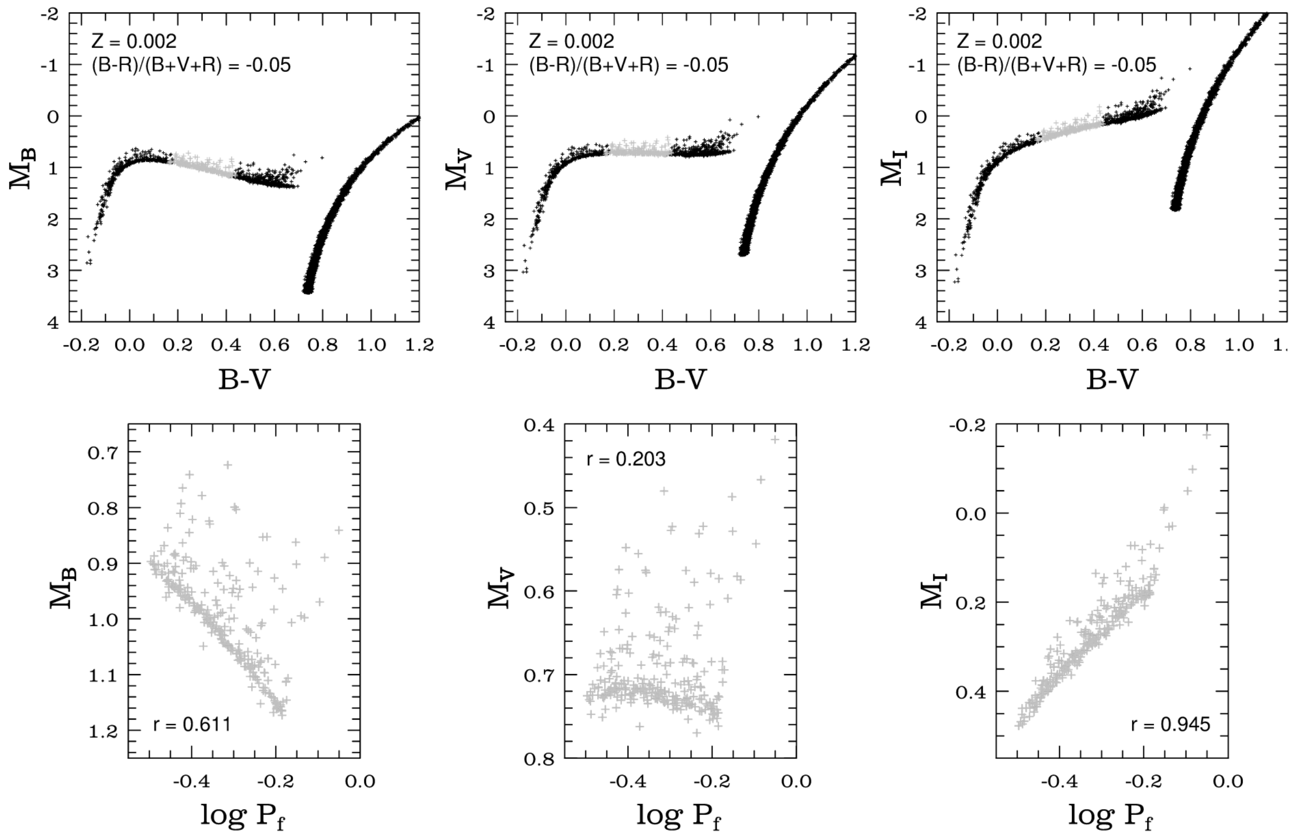

HB simulation with Z= 0.001 and an intermediate HB type, Catelan=2004

Period-luminosity(-metallicity) relations for RR Lyrae variable hold only in the infrared bands

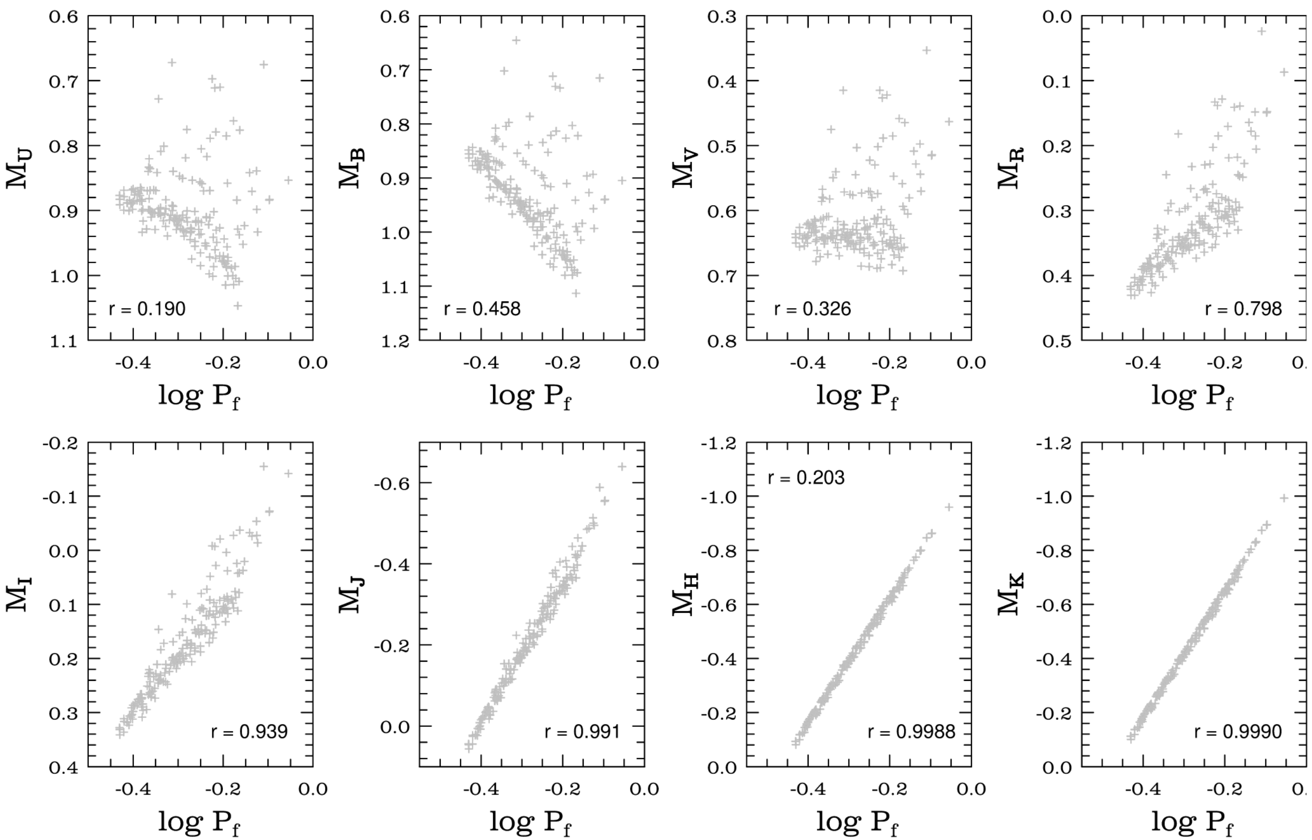

HB simulation with Z= 0.001 and an intermediate HB type, Catelan=2004

Major role of the bolometric correction (BC).

The BCs in the optical regime almost constant when moving from the blue to the red edge of the instability strip, while in the NIR regime they increases.

This means that regular variables in the NIR become intrinsically brighter when moving from hotter (shorter periods) to cooler (longer periods) variables.

→ Completely different physical origin of PL relations compared with Cepheids

Period-luminosity(-metallicity) relations for RR Lyrae variable hold only in the infrared bands

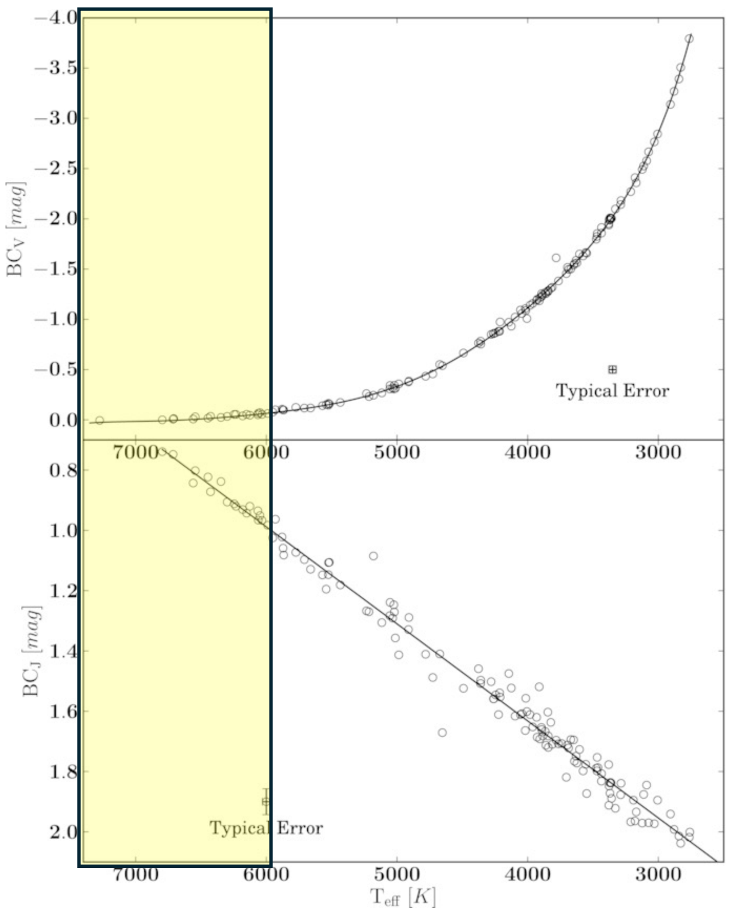

Pecaut+2013

Major role of the bolometric correction (BC).

The BCs in the optical regime almost constant when moving from the blue to the red edge of the instability strip.

In the NIR regime they increases →

Variables in the NIR become intrinsically brighter when moving from hotter (shorter periods) to cooler (longer periods) variables.

Theory predicts a metallicity term

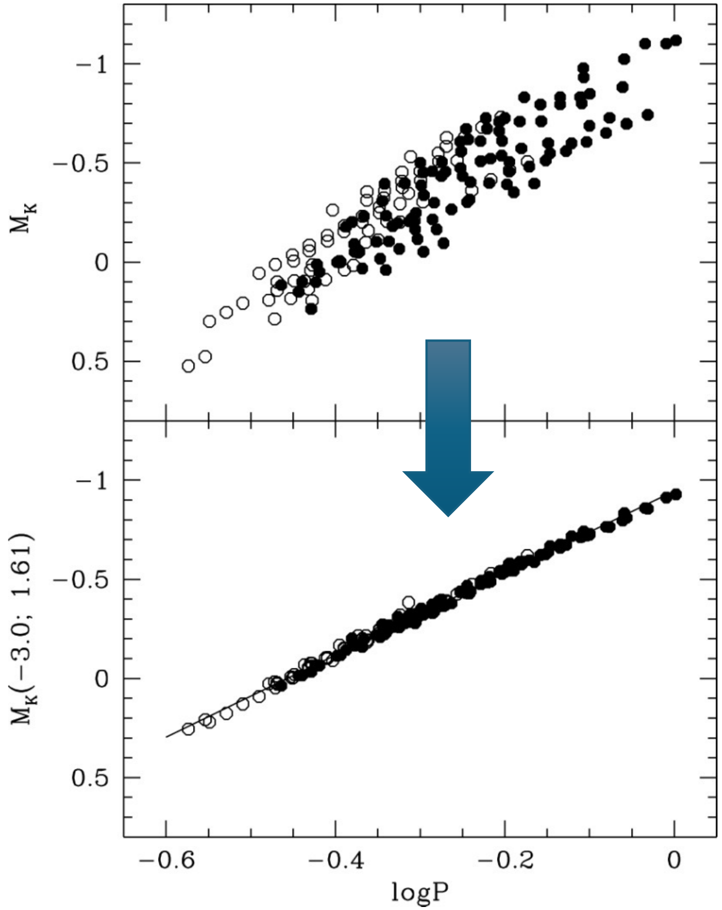

Bono et al. 2001 MNRAS

Correcting for metallicity differences and evolutionary effects the dispersion is significantly decreased !

The true relation is of the form

$M_K = a + b \log P + c\,[Fe/H]$

Tight PLZ_K relation: $\sigma \sim 0.05$ mag

$M_K = -0.82 - 2.25 \log P + 0.18\,[Fe/H]$

(Marconi+2015)

Observed PLK-[Fe/H]

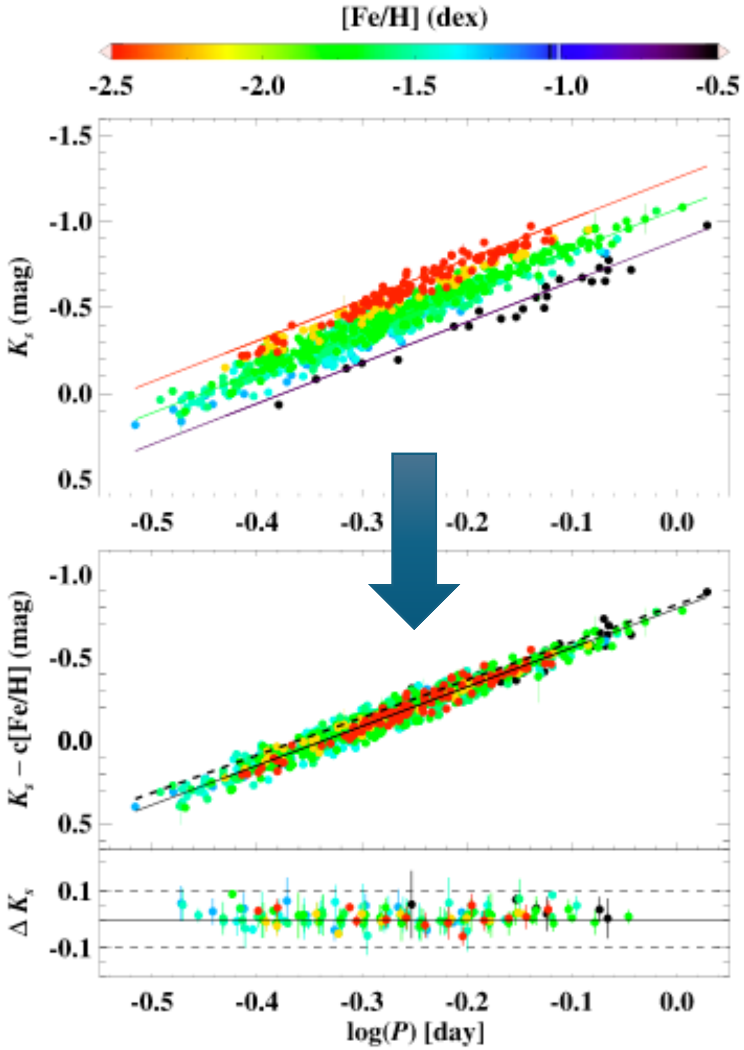

Observed metallicity coefficients are consistent with the pulsational model predictions

Bhardwaj+2023

The predicted Period-Wesenheit relations for RR Lyrae stars

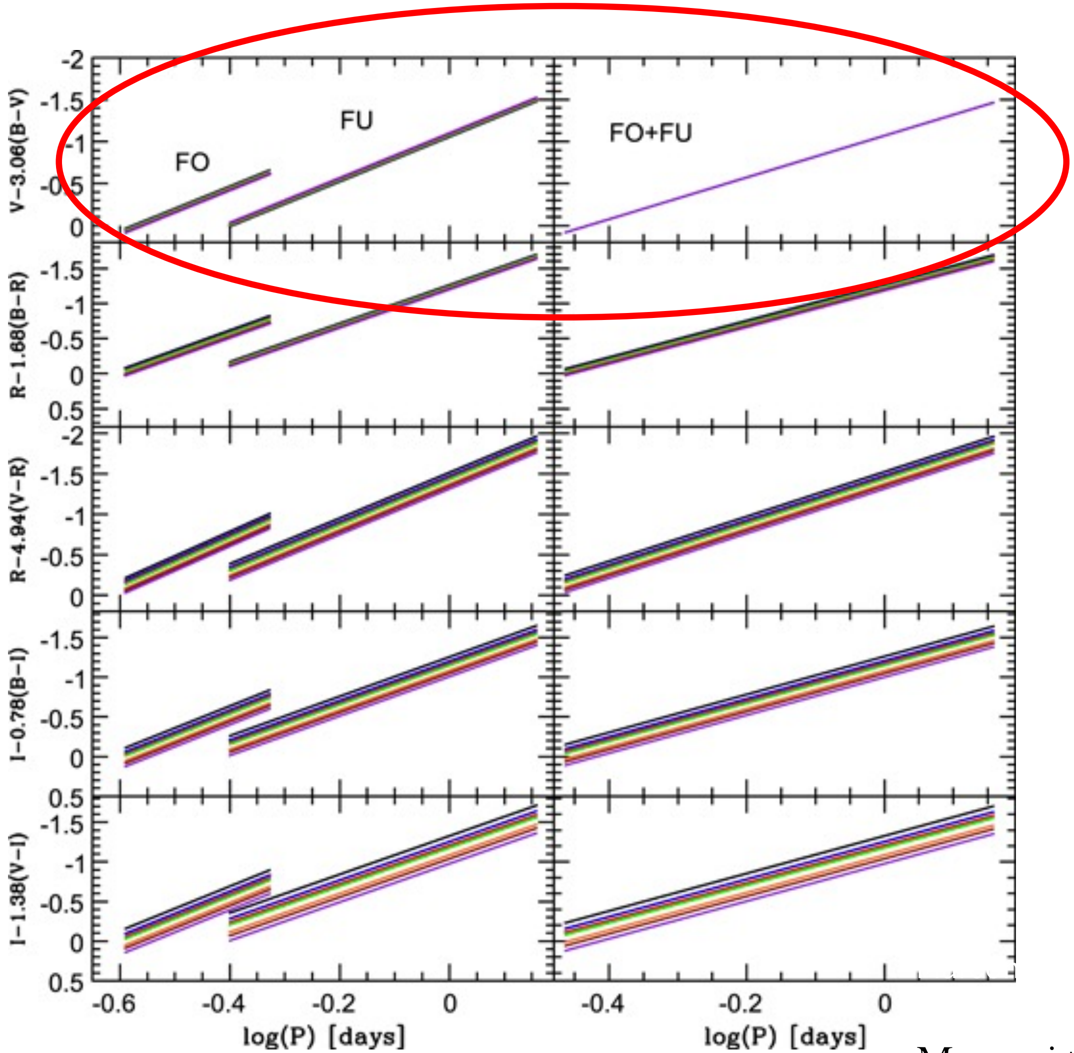

Period-Wesenheit relations for RR Lyrae variables also hold in the optical: W depends on colour, hence on period

The combination W(V,B-V) is the least sensitive to metallicity.

Marconi+ 2017 ApJ

The observed Period-Wesenheit relations for RR Lyrae stars

Good agreement with pulsational model predictions

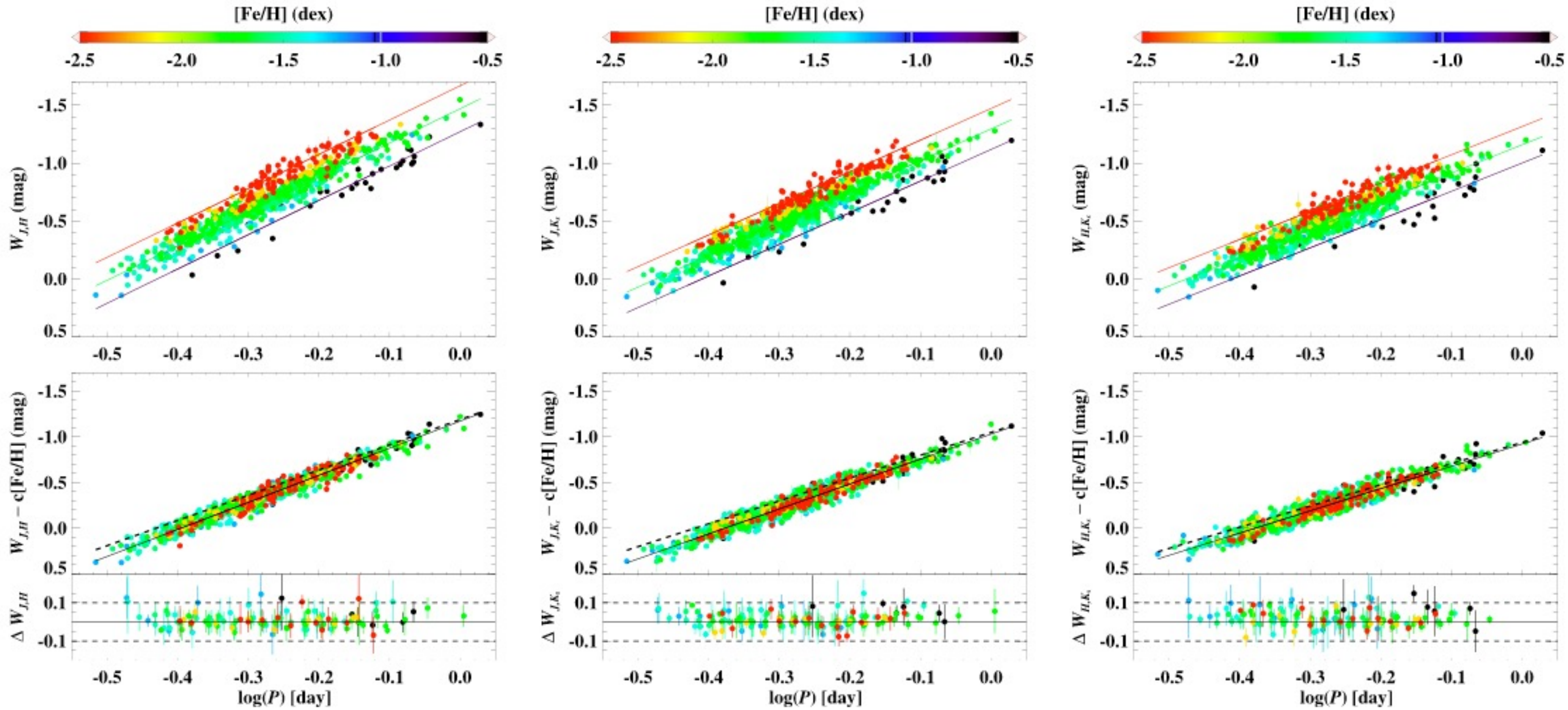

Bhardwaj+2023